Modulating Exciton Dissociation and Charge Transfer by Extending π-conjugation in Thiazole-based COFs to Boost Photocatalytic Hydrogen Evolution

Jianing Tang[a], Jinfeng Wang*[a], Ziang Song[a], Man Wang[a], Haitao Song[a], Yujun Xie*[a] and Zhen Li*[a, b, c]

[a] Institute of Molecular Aggregation Science, Tianjin University, Tianjin 300072, China

Emails: jinfeng.wang@tju.edu.cn, xieyujun@tju.edu.cn, lizhen@whu.edu.cn.

[b] Hubei Key Lab on Organic and Polymeric Opto-Electronic Materials, Department of Chemistry, Wuhan University, Wuhan, Hubei, 430072, China

Email: lizhen@whu.edu.cn.

[c] College of Chemistry and Chemical Engineering, Hubei University, Wuhan 430072, China

Table of Contents

Section I. Synthetic procedures

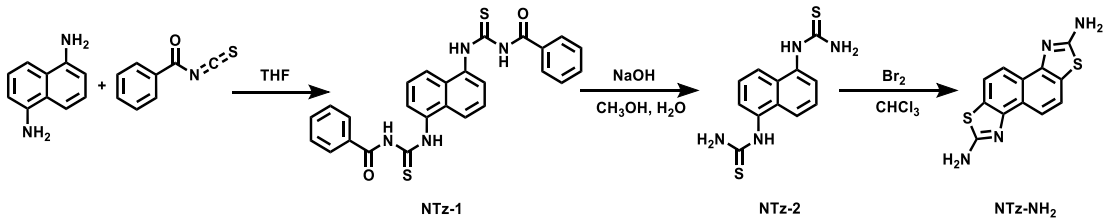

Fig. S1. The synthetic route of NTz-NH_2.

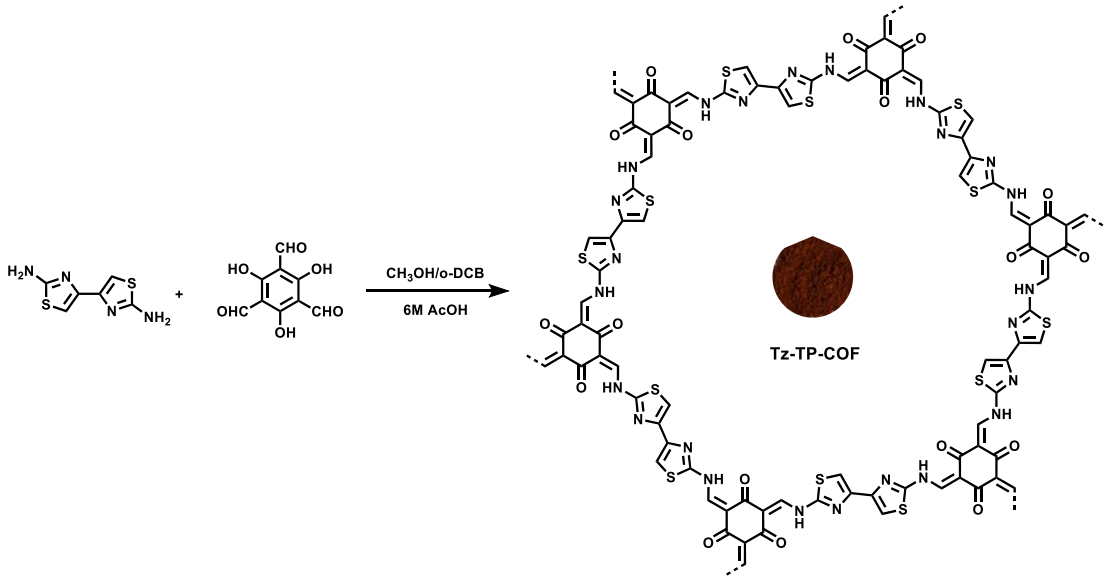

Fig. S2. The synthetic route of Tz-TP-COF.

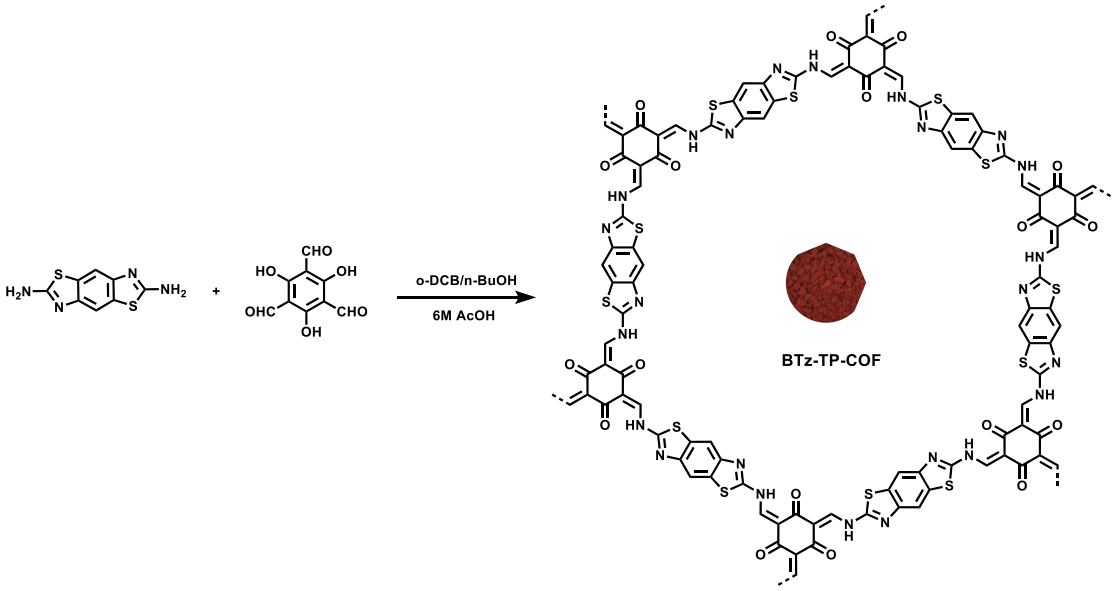

Fig. S3. The synthetic route of BTz-TP-COF.

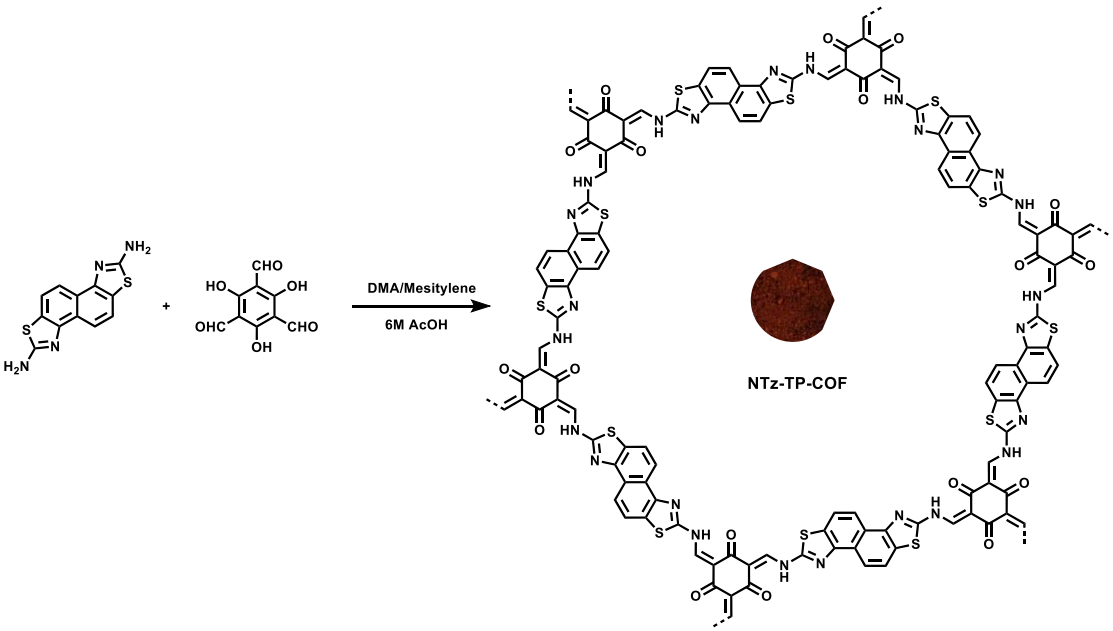

Fig. S4. The synthetic route of NTz-TP-COF.

Section II. Supplementary figures and tables

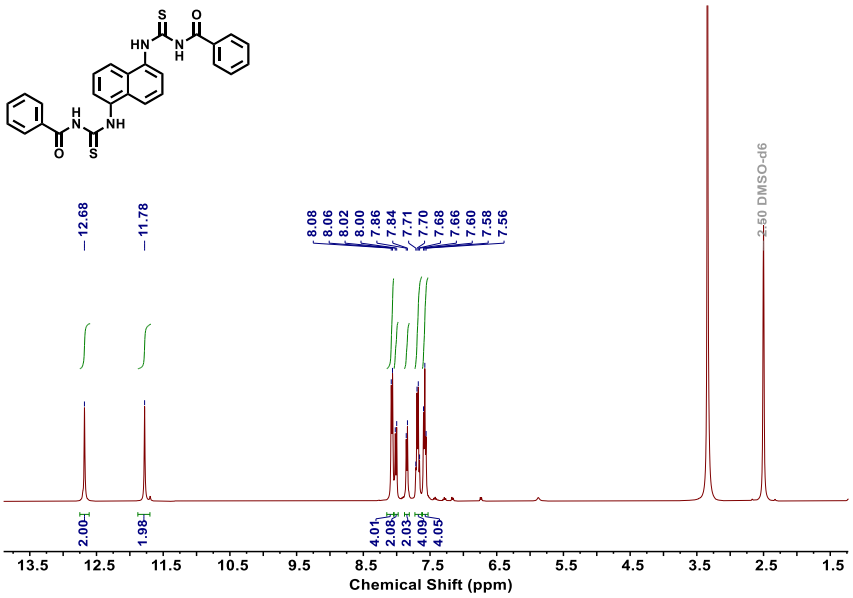

Fig. S5. ^{1}H NMR spectrum of NTz-1.

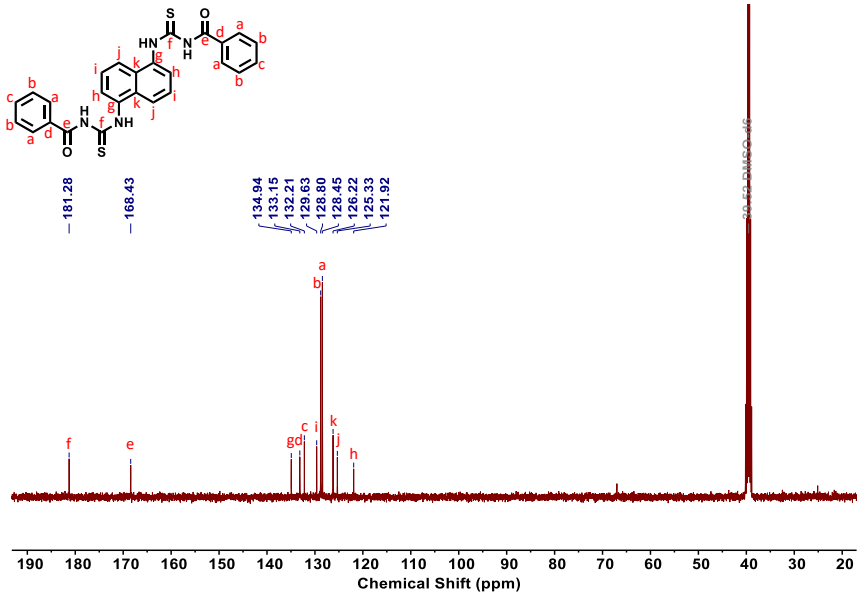

Fig. S6. ^{13}C NMR spectrum of NTz-1.

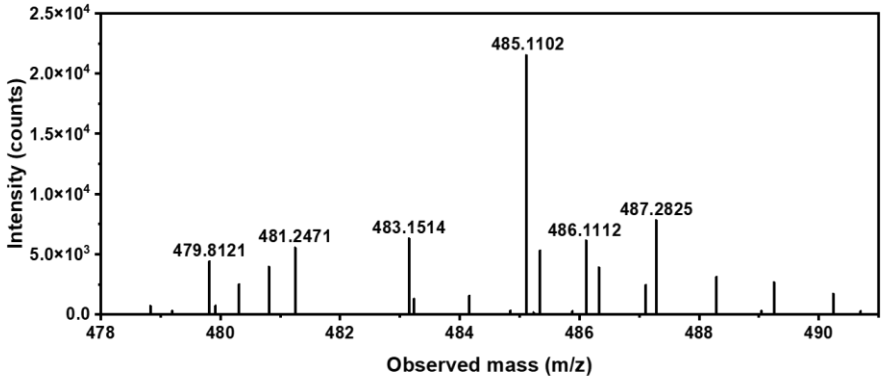

Fig. S7. HRMS spectrum of NTz-1.

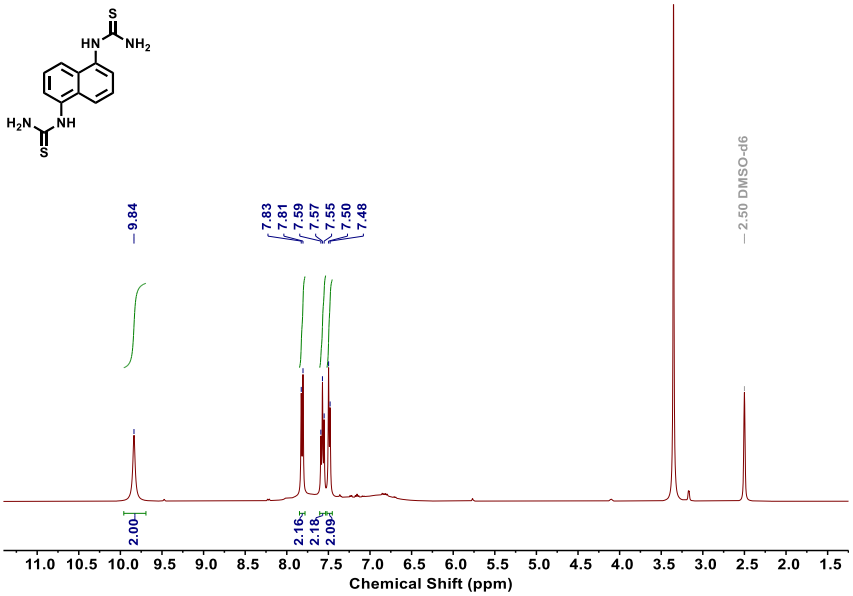

Fig. S8. ^{1}H NMR spectrum of NTz-2.

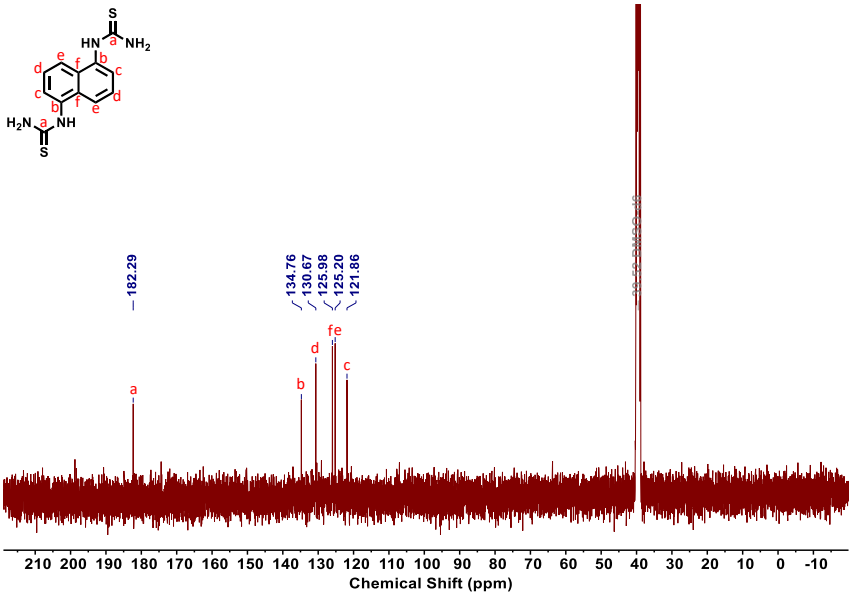

Fig. S9. ^{13}C NMR spectrum of NTz-2.

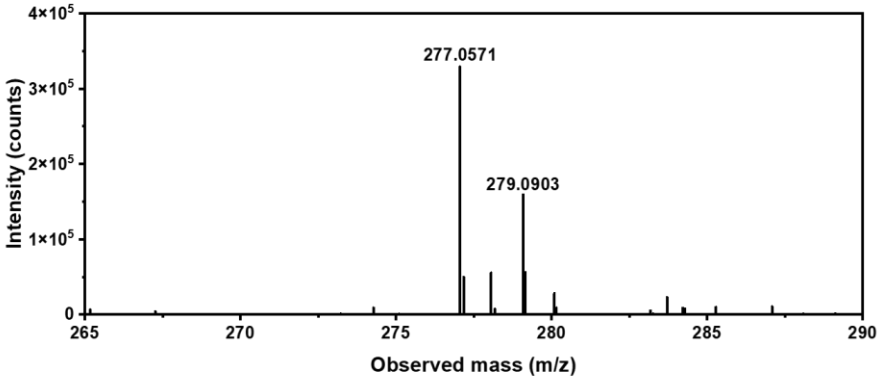

Fig. S10. HRMS spectrum of NTz-2.

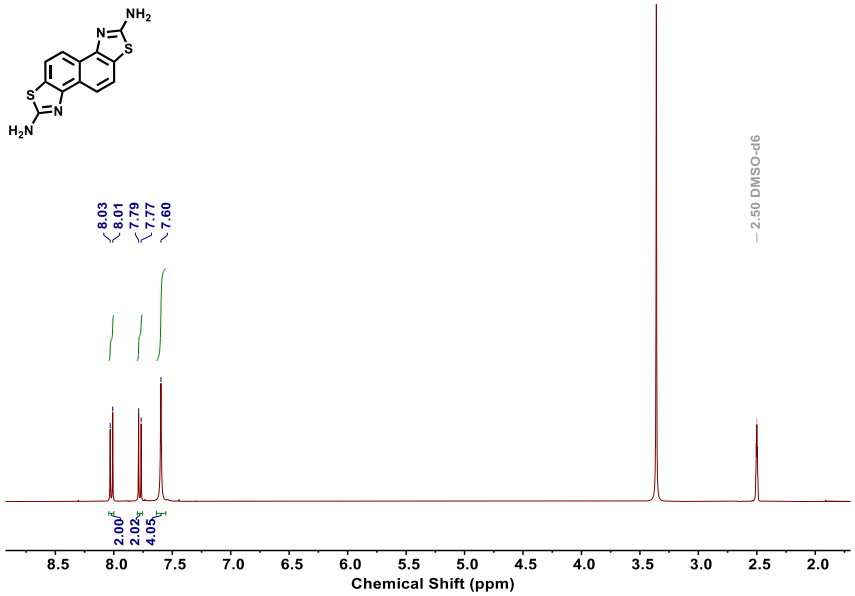

Fig. S11. ^{1}H NMR spectrum of NTz-NH_2.

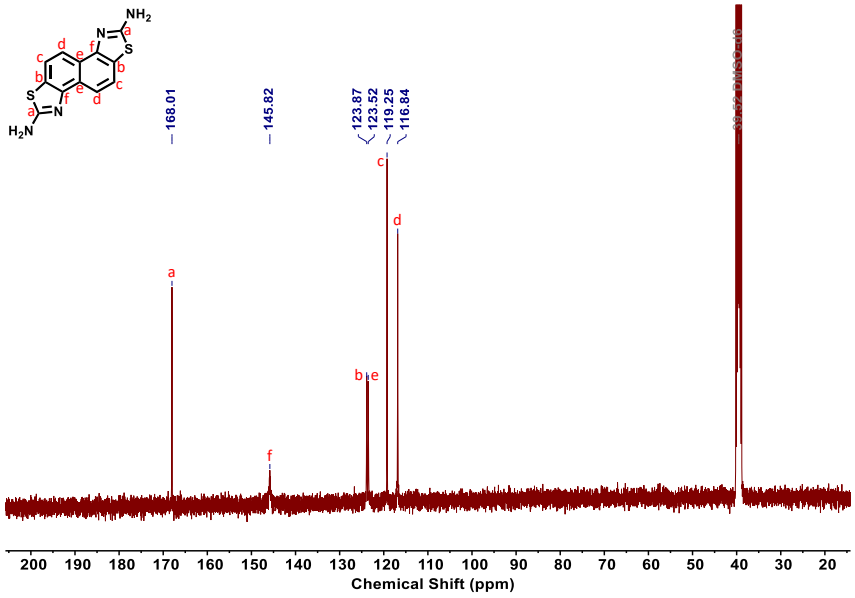

Fig. S12. ^{13}C NMR spectrum of NTz-NH_2.

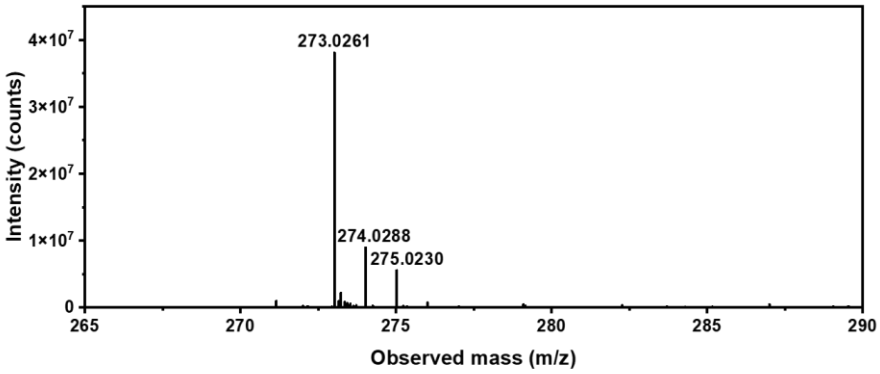

Fig. S13. HRMS spectrum of NTz-NH_2.

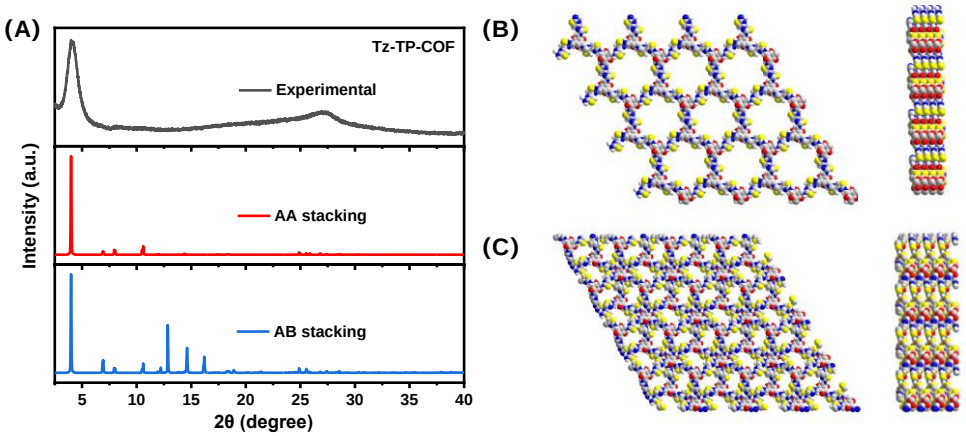

Fig. S14. (A) The experimental, simulated AA stacking, simulated AB stacking of Tz-TP-COF. (B) Top view and side view of simulated AA stacking. (C) Top view and side view of simulated AB stacking.

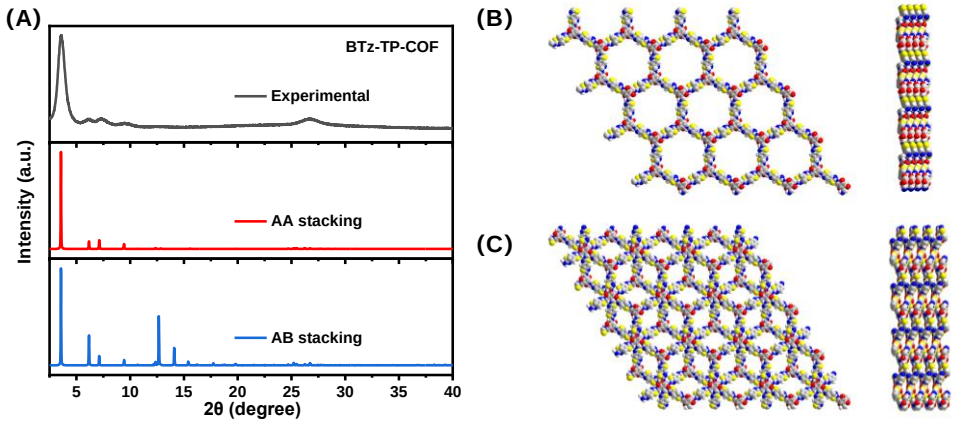

Fig. S15. (A) The experimental, simulated AA stacking, simulated AB stacking of BTz-TP-COF. (B) Top view and side view of simulated AA stacking. (C) Top view and side view of simulated AB stacking.

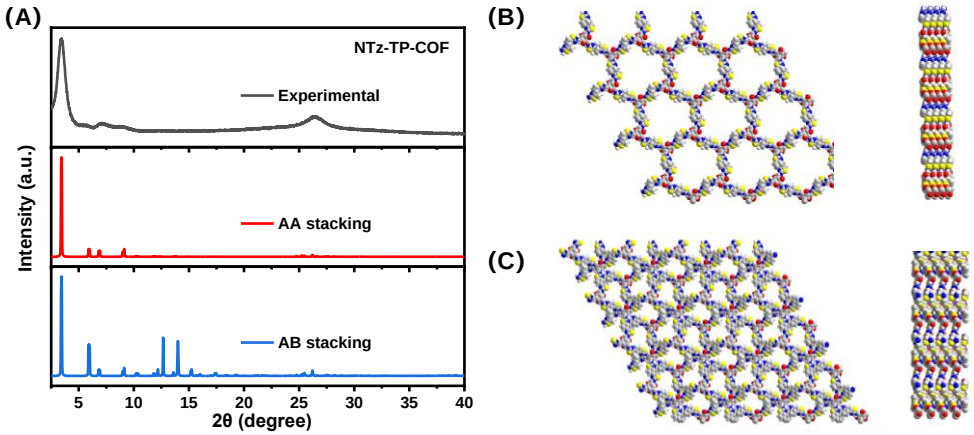

Fig. S16. (A) The experimental, simulated AA stacking, simulated AB stacking of NTz-TP-COF. (B) Top view and side view of simulated AA stacking. (C) Top view and side view of simulated AB stacking.

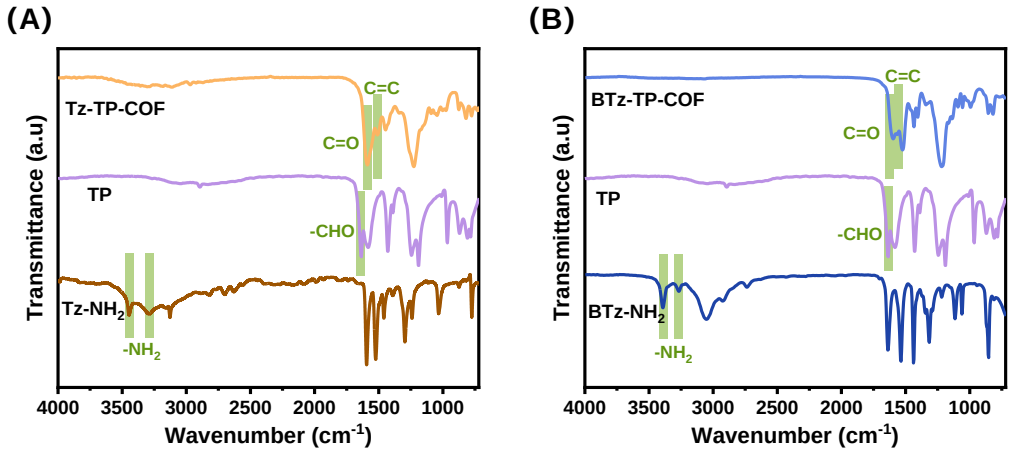

Fig. S17. FT-IR spectra of (A) Tz-TP-COF, TP and Tz-NH_2, (B) BTz-TP-COF, TP and BTz-NH_2.

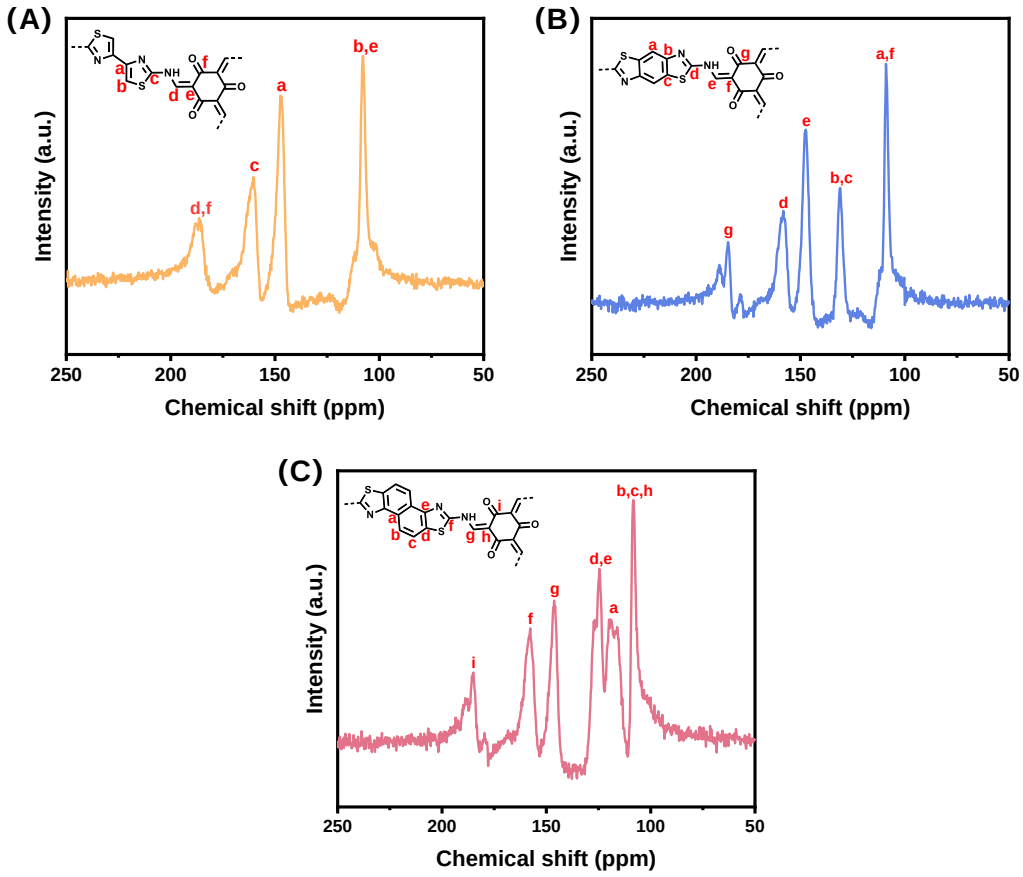

Fig. S18. Solid state ^{13}C CP/MAS NMR spectra of (A) Tz-TP-COF, (B) BTz-TP-COF and (C) NTz-TP-COF.

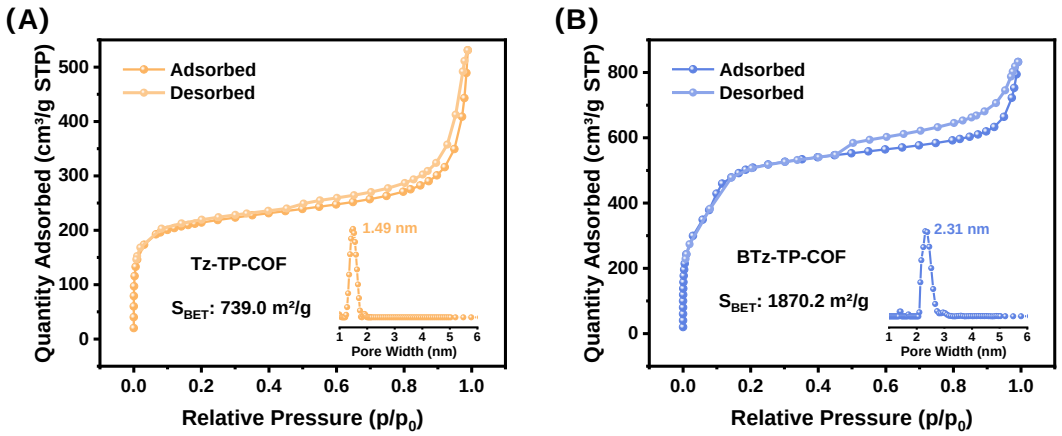

Fig. S19. (A) N_2 adsorption-desorption isotherm of Tz-TP-COF at 77 K (adsorption: deep orange; desorption: light orange). Inset: Pore size distribution curve. (B) N_2 adsorption-desorption isotherm of BTz-TP-COF at 77 K (adsorption: deep blue; desorption: light blue). Inset: Pore size distribution curve.

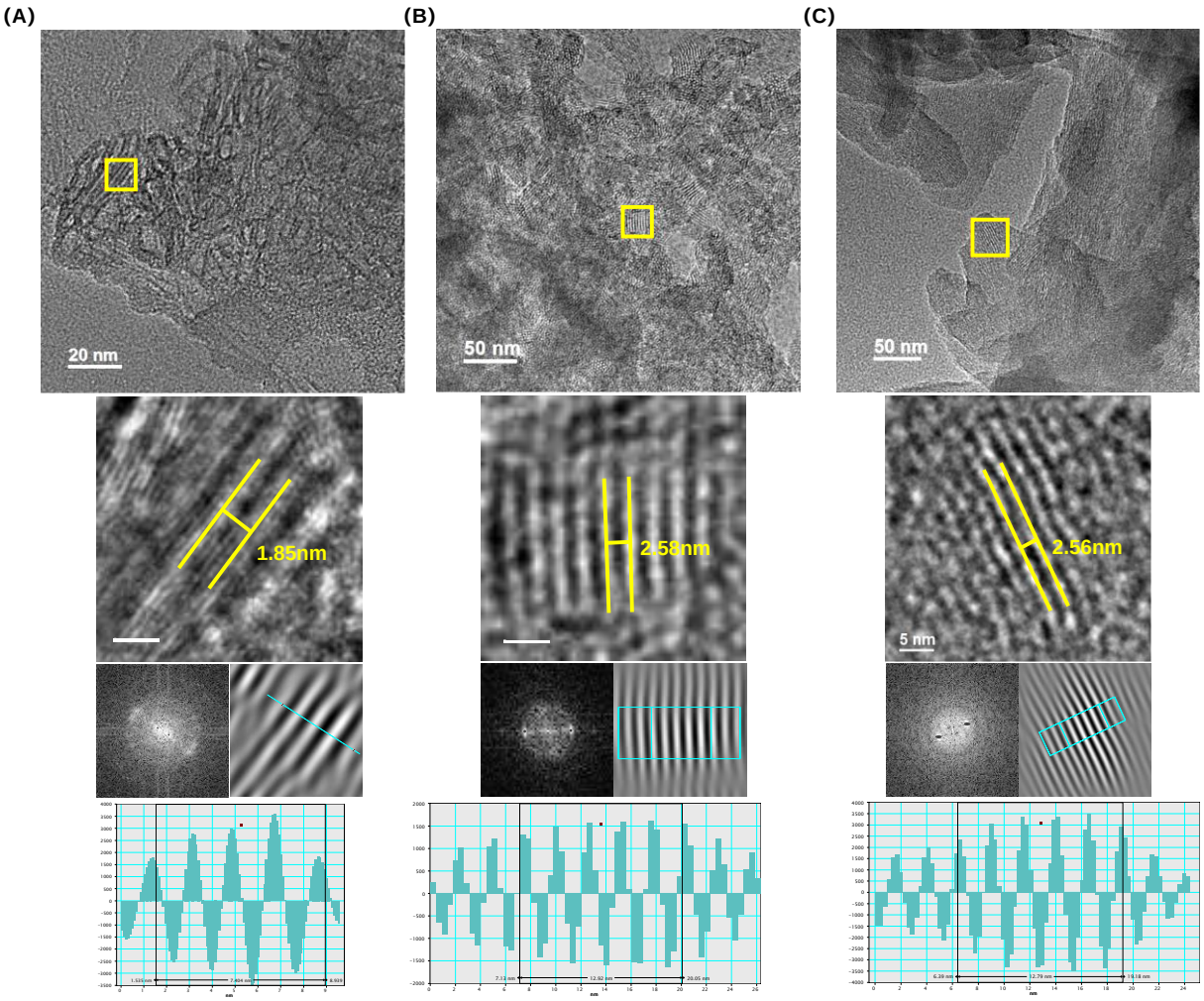

Fig. S20. High-resolution TEM image, Fast Fourier transform of HRTEM and crystal lattice spacing of (A) Tz-TP-COF, (B) BTz-TP-COF and (C) NTz-TP-COF.

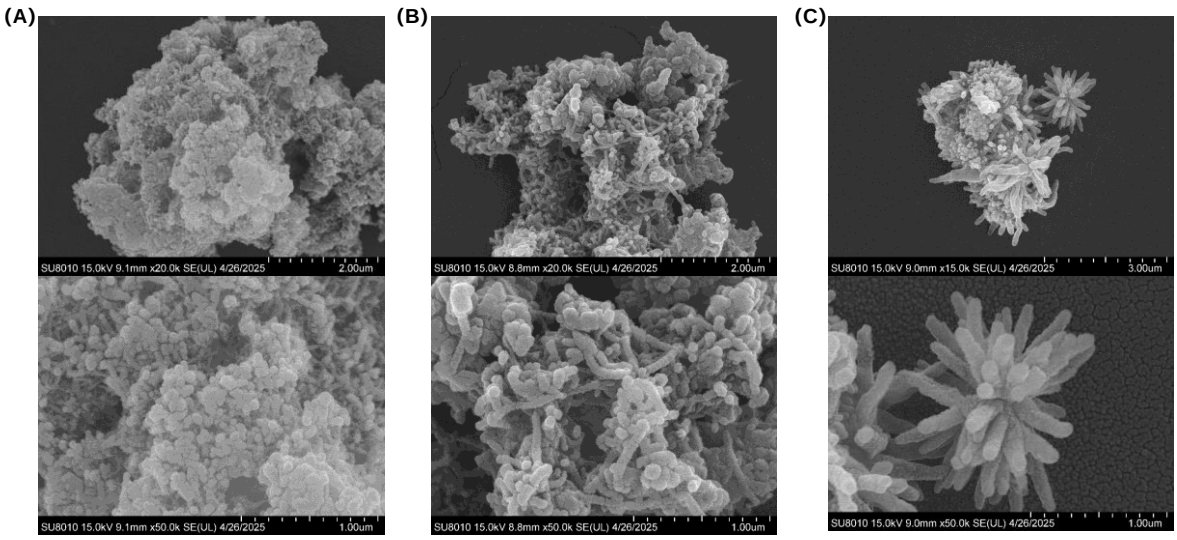

Fig. S21. SEM images of (A) Tz-TP-COF, (B) BTz-TP-COF and (C) NTz-TP-COF.

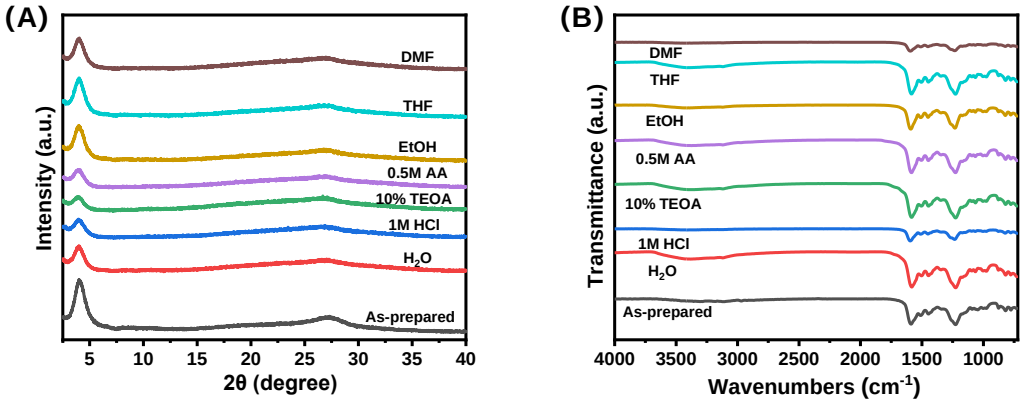

Fig. S22. (A) PXRD pattern and (B) FT-IR spectra of Tz-TP-COF after various treatments for 24 h.

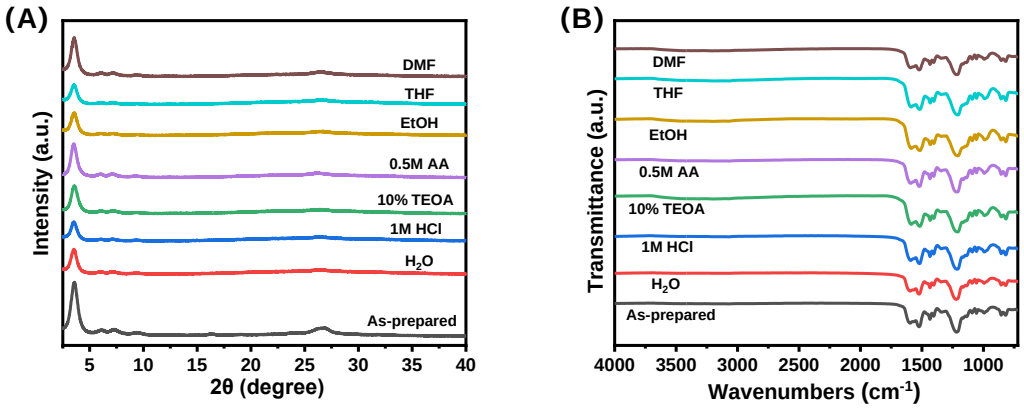

Fig. S23. (A) PXRD pattern and (B) FT-IR spectra of BTz-TP-COF after various treatments for 24 h.

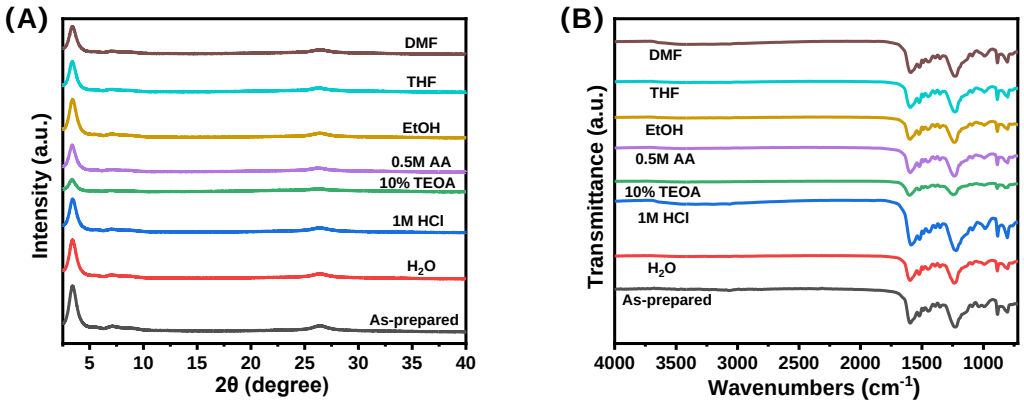

Fig. S24. (A) PXRD pattern and (B) FT-IR spectra of NTz-TP-COF after various treatments for 24 h.

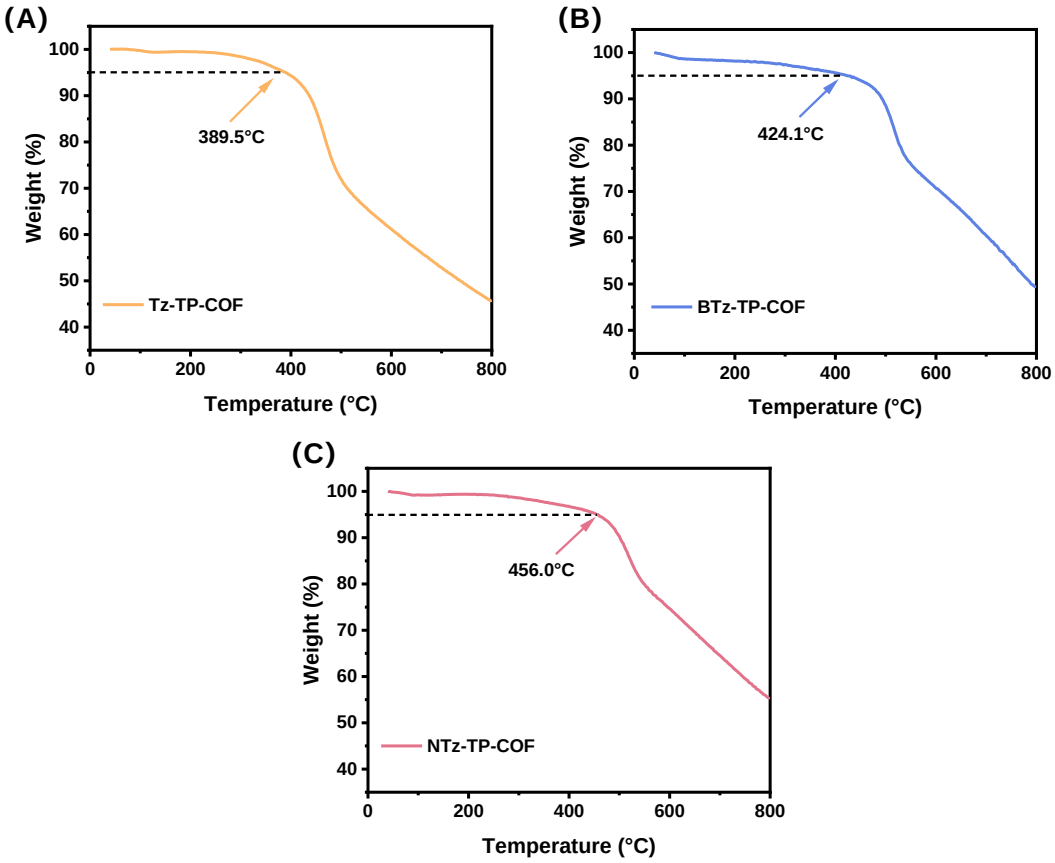

Fig. S25. TGA profiles of (A) Tz-TP-COF, (B) BTz-TP-COF and (C) NTz-TP-COF.

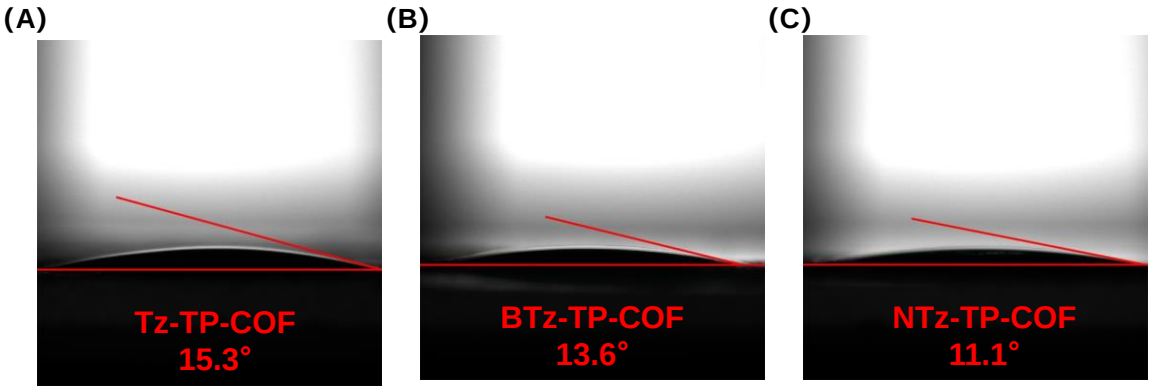

Fig. S26. Contact angles of (A) Tz-TP-COF, (B) BTz-TP-COF and (C) NTz-TP-COF.

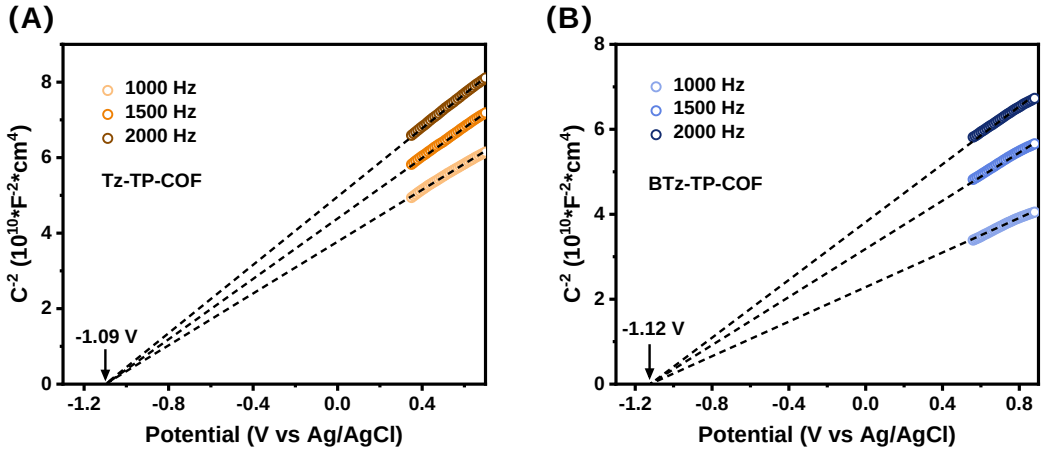

Fig. S27. Mott-Schottky (M-S) plot for Tz-TP-COF(A) and BTz-TP-COF(B) measured in Na_2SO_4 (0.2 M, pH = 6.8) with Ag/AgCl electrode as the reference electrode in dark.

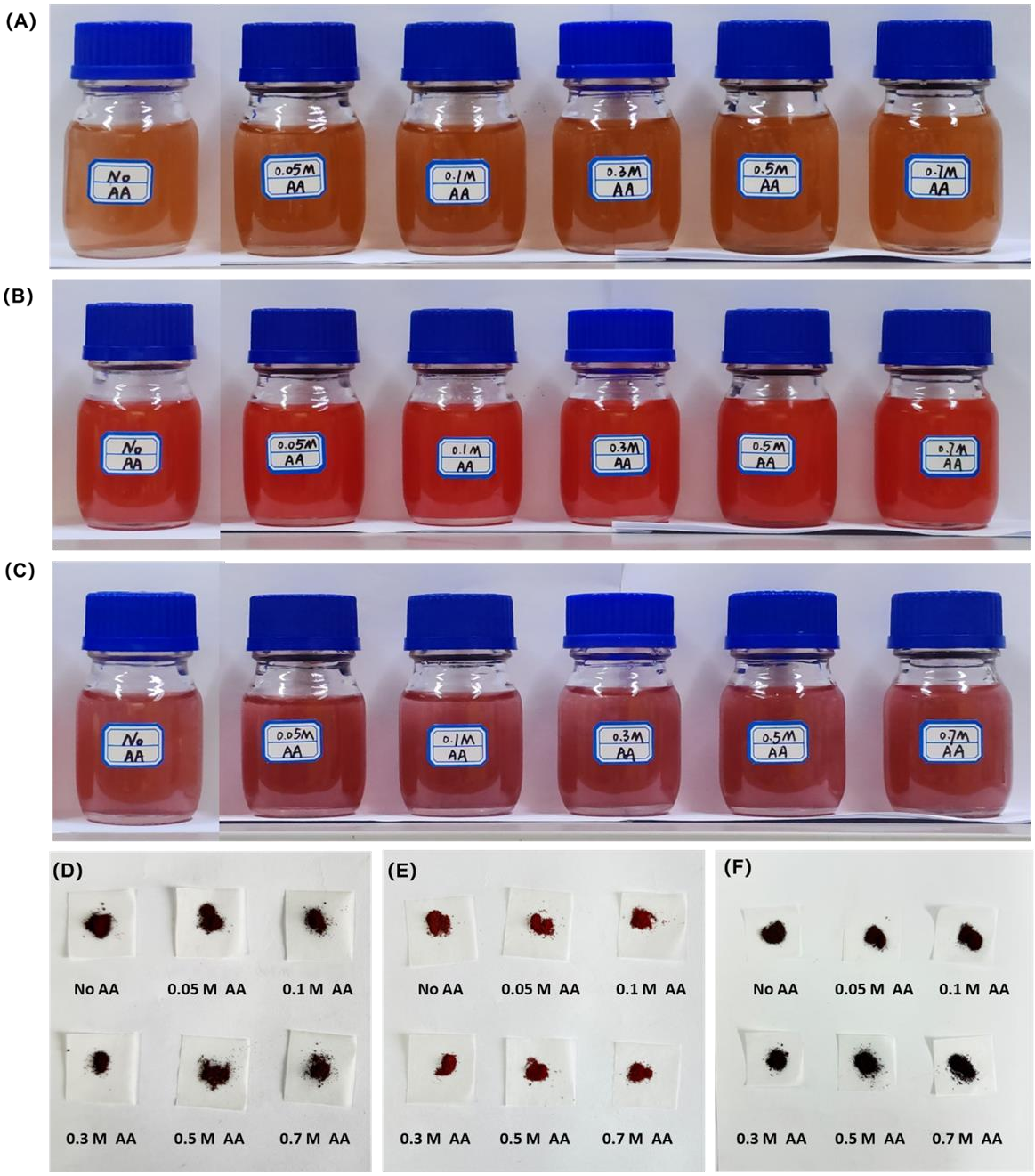

Fig. S28. (A-C) Dispersions of 5 mg Tz-TP-COF (A), BTz-TP-COF (B), and NTz-TP-COF (C) in deionized water, 0.05 M AA, 0.1 M AA, 0.3 M AA, 0.5 M AA, and 0.7 M AA solutions, respectively. (D-F) Tz-TP-COF (D), BTz-TP-COF (E), and NTz-TP-COF (F) obtained by filtration after immersion in the different concentrations of AA solutions.

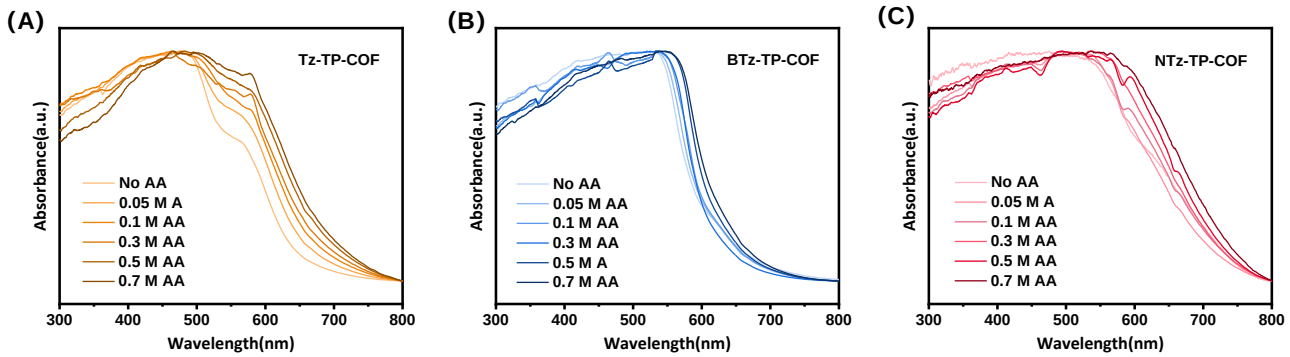

Fig. S29. UV-Vis DRS of Tz-TP-COF (A), BTz-TP-COF (B), and NTz-TP-COF (C) before and after protonation.

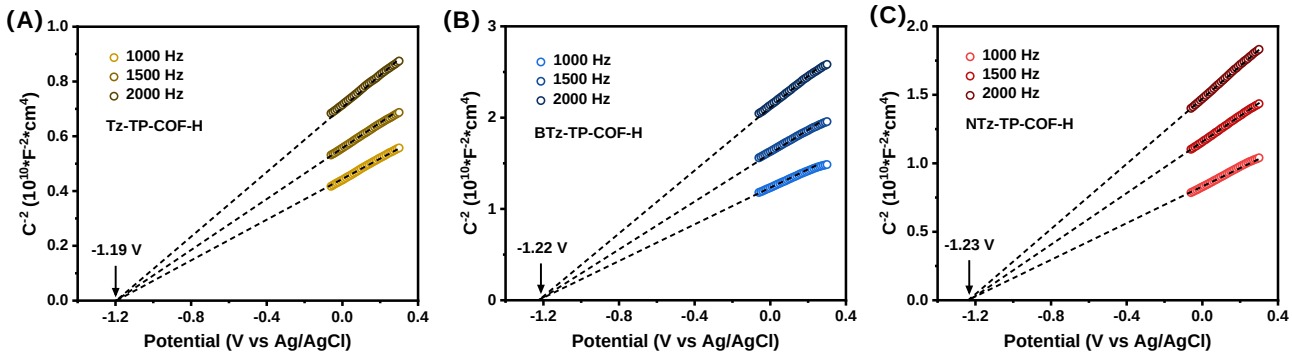

Fig. S30. Mott-Schottky (M-S) plots for Tz-TP-COF (A), BTz-TP-COF (B) and NTz-TP-COF (C) measured in an electrolyte consisting of 0.5 M AA and 0.2 M Na_2SO_4 (pH = 2.4), using an Ag/AgCl reference electrode, under dark conditions.

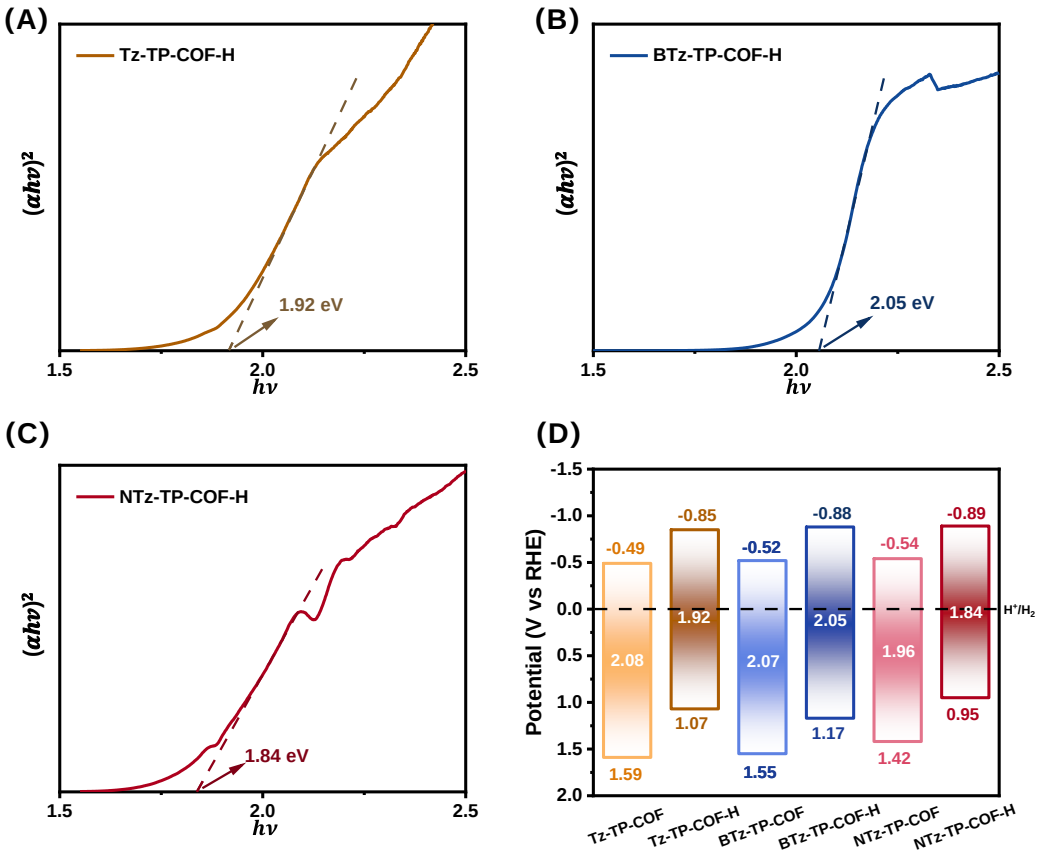

Fig. S31. (A-C) Bandgaps of Tz-TP-COF (A), BTz-TP-COF (B), and NTz-TP-COF (C) calculated using the Tauc plot method after protonation in 0.5 M AA. (D) Comparative electronic band structures of Tz-TP-COF, BTz-TP-COF, and NTz-TP-COF before and after protonation with 0.5 M AA.

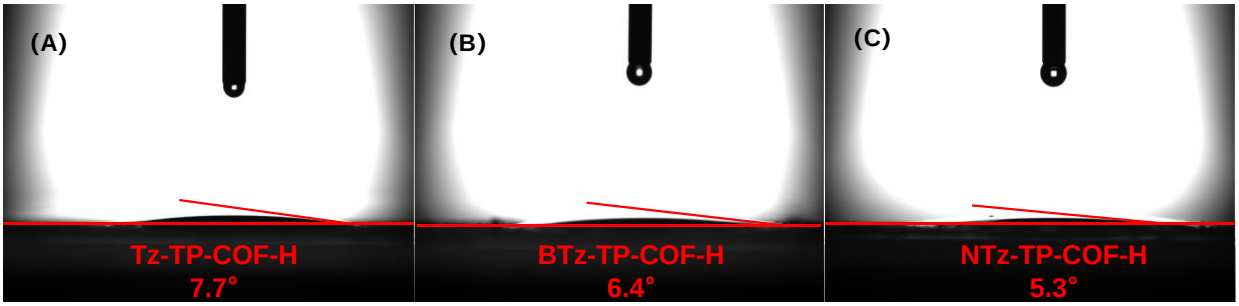

Fig. S32. Contact angles of Tz-TP-COF (A), BTz-TP-COF (B), and NTz-TP-COF (C) after immersion in 0.5 M AA.

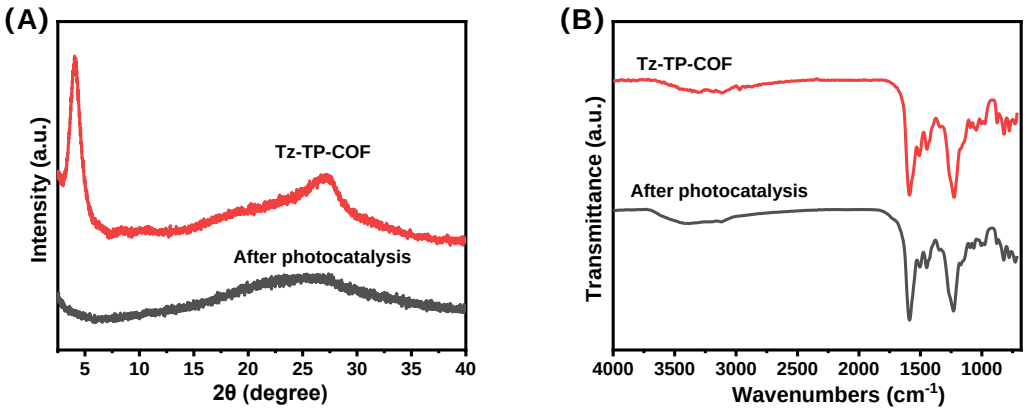

Fig. S33. (A) PXRD patterns and (B) FT-IR spectra of 5mg Tz-TP-COF before and after the cyclic hydrogen evolution reaction test.

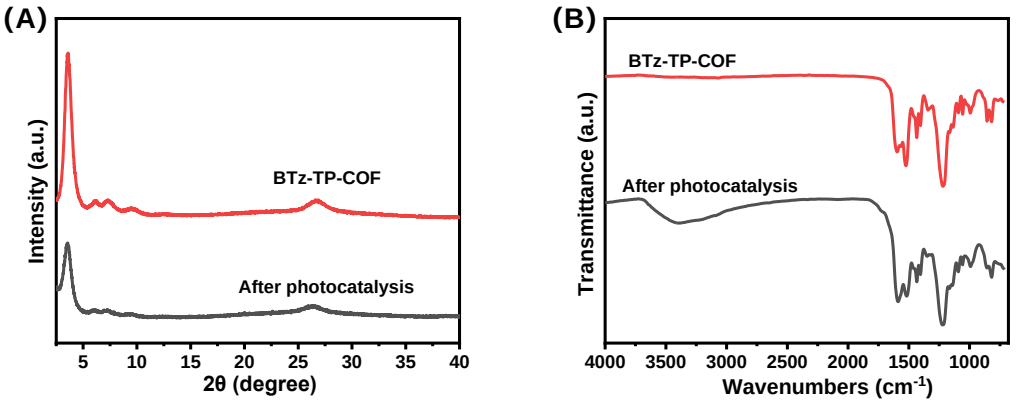

Fig. S34. (A) PXRD patterns and (B) FT-IR spectra of 5mg BTz-TP-COF before and after the cyclic hydrogen evolution reaction test.

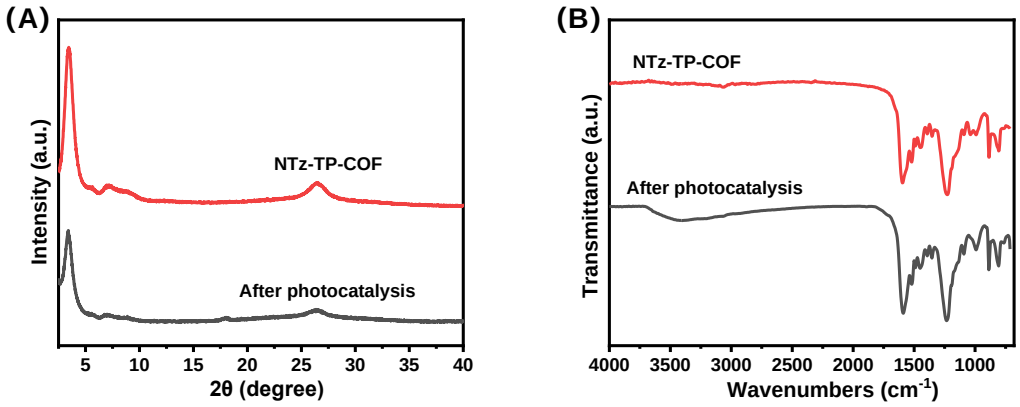

Fig. S35. (A) PXRD patterns and (B) FT-IR spectra of 5mg NTz-TP-COF before and after the cyclic hydrogen evolution reaction test.

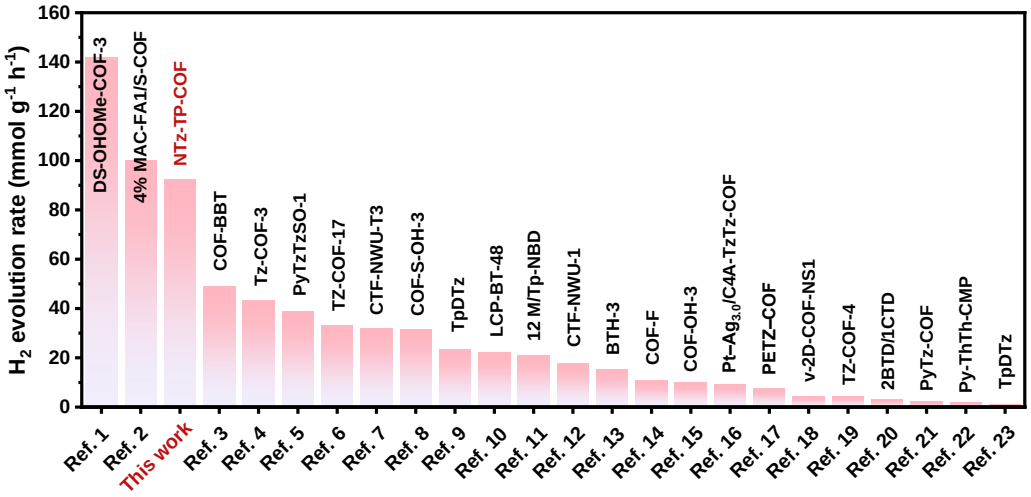

Fig. S36. Comparison of the photocatalytic hydrogen evolution performance in water of NTz-TP-COF with other representative thiazole-based and TP based conjugated polymer photocatalysts reported in the literature.[1-23]

Table S1. Hydrogen evolution rates of the three COFs from repeated experiments

Sample	HER (mmol g^{-1} h^{-1})				Mean ± SD
	1	2	3	4	
Tz-TP-COF	4.70	5.55	5.50	4.10	4.96 ± 0.69
BTz-TP-COF	29.15	31.60	29.55	35.05	31.34 ± 2.70
NTz-TP-COF	92.30	91.95	87.95	89.50	90.43 ± 2.07

Experiments conditions: 2 mg COF, 0.5 M AA, 3 wt% Pt, λ > 420 nm.

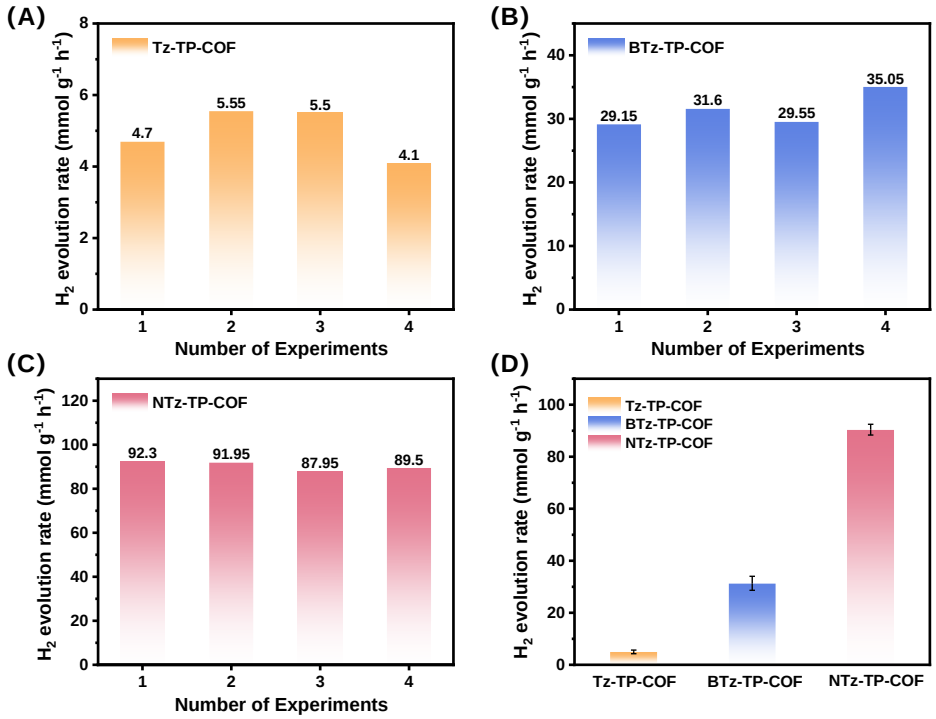

Fig. S37. (A-C) Photocatalytic hydrogen evolution rates of Tz-TP-COF (A), BTz-TP-COF (B), and NTz-TP-COF (C) from four independent photocatalytic experiments. (D) Average hydrogen evolution rates of the three COFs (with error bars). Experimental conditions: 2 mg COF, 0.5 M AA, 3 wt% Pt.

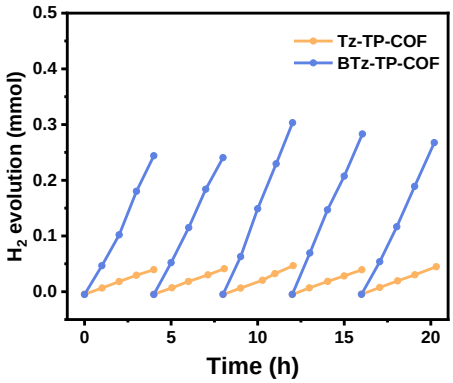

Fig. S38. Cycling tests over 20 h for 2 mg COFs as photocatalysts under visible light, with 0.5 M AA as sacrificial agent and 3 wt% Pt as co-catalyst.

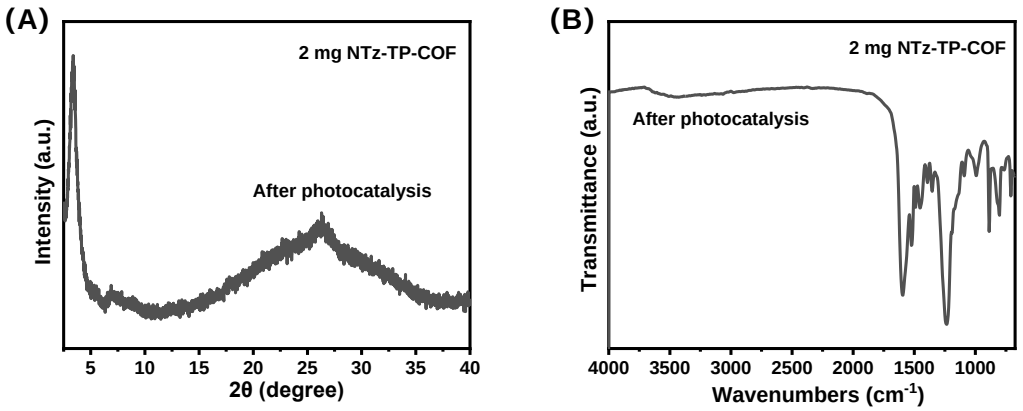

Fig. S39 (A) PXRD pattern and (B) FT-IR spectrum of 2mg NTz-TP-COF after cyclic hydrogen evolution reaction testing.

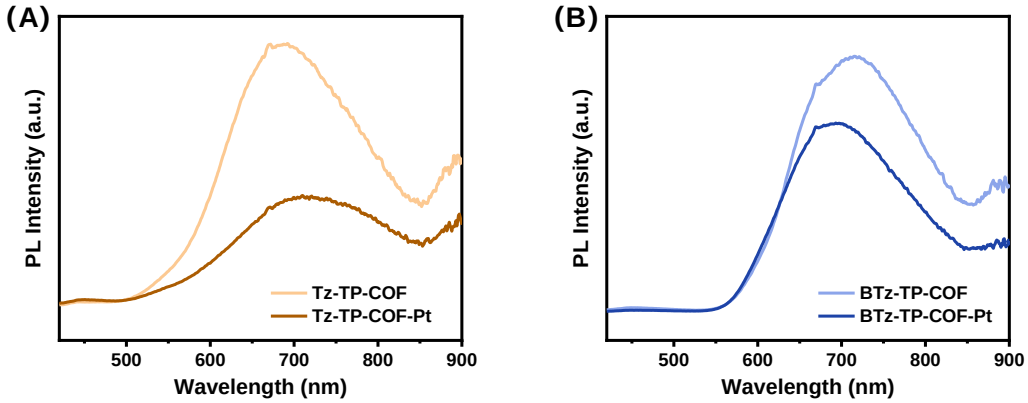

Fig. S40. (A) Steady-state photoluminescence (PL) spectra of Tz-TP-COF before and after Pt photodeposition. (B) Steady-state photoluminescence (PL) spectra of BTz-TP-COF before and after Pt photodeposition.

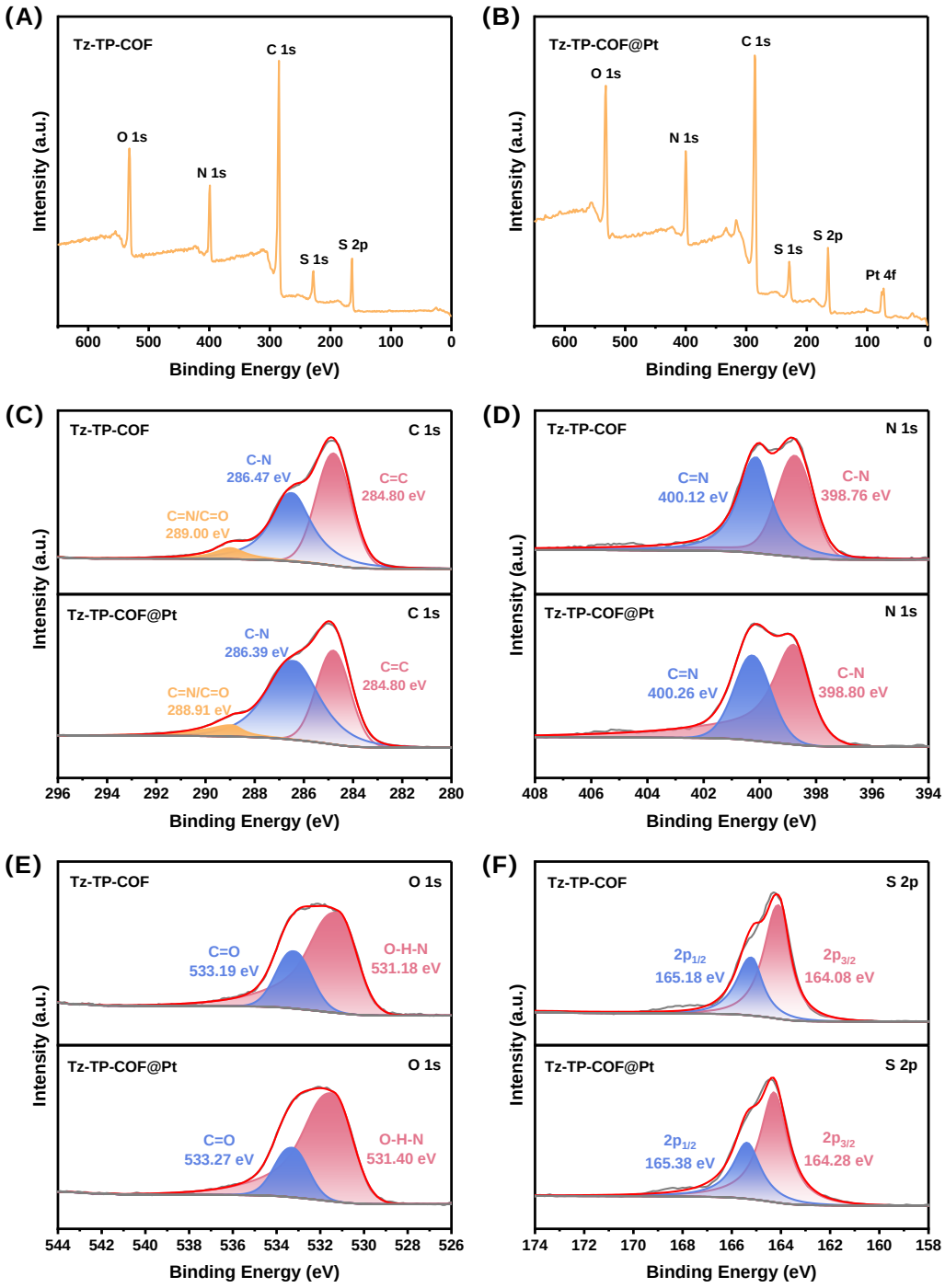

Fig. S41. (A) XPS survey spectra of Tz-TP-COF before photocatalysis. (B) XPS survey spectra of Tz-TP-COF after photocatalysis. (C) High resolution XPS spectra of C 1s for Tz-TP-COF before and after photocatalysis. (D) High resolution XPS spectra of N 1s for Tz-TP-COF before and after photocatalysis. (E) High resolution XPS spectra of O 1s for Tz-TP-COF before and after photocatalysis. (F) High resolution XPS spectra of S 2p for Tz-TP-COF before and after photocatalysis.

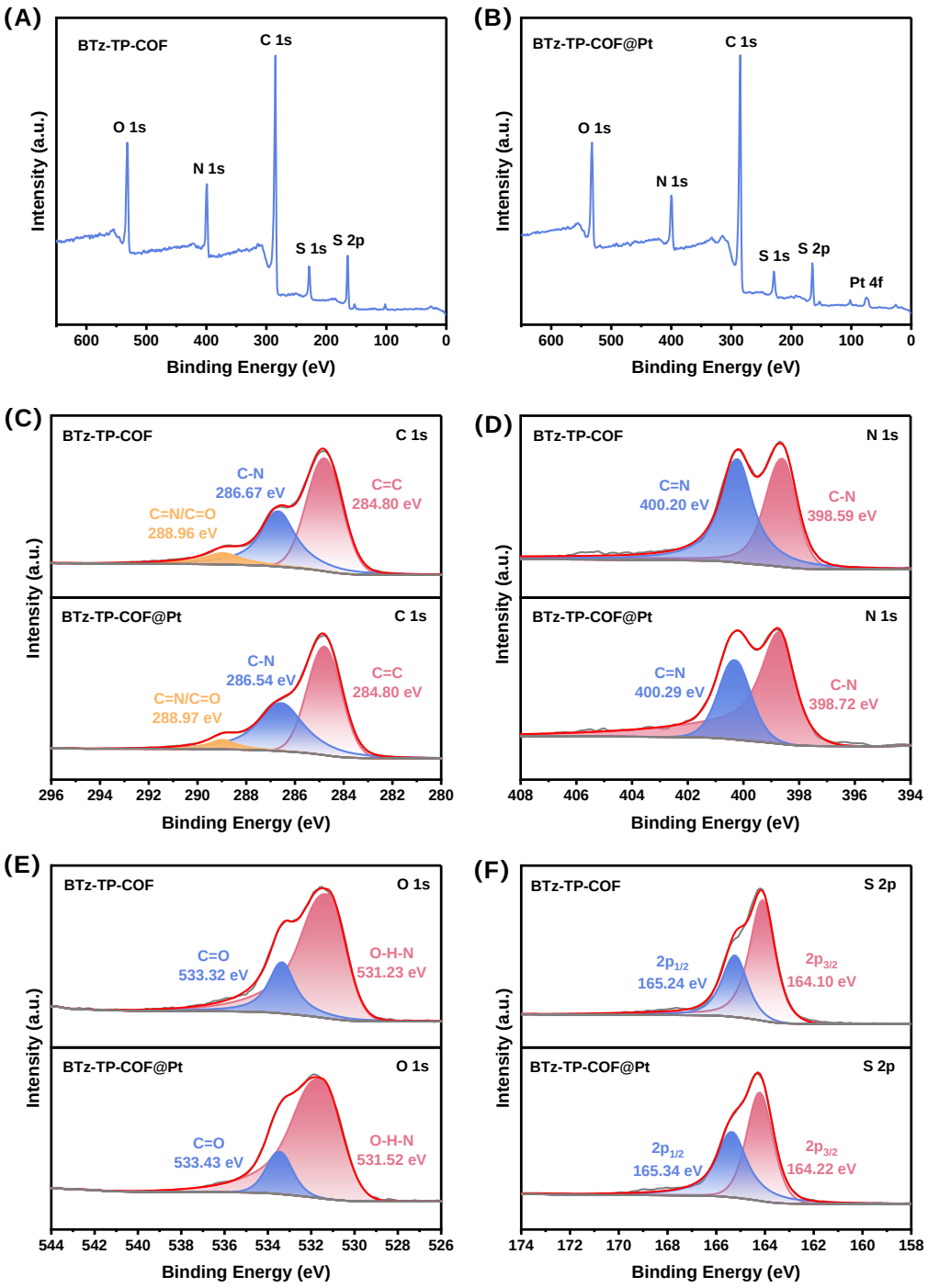

Fig. S42. (A) XPS survey spectra of BTz-TP-COF before photocatalysis. (B) XPS survey spectra of BTz-TP-COF after photocatalysis. (C) High resolution XPS spectra of C 1s for BTz-TP-COF before and after photocatalysis. (D) High resolution XPS spectra of N 1s for BTz-TP-COF before and after photocatalysis. (E) High resolution XPS spectra of O 1s for BTz-TP-COF before and after photocatalysis. (F) High resolution XPS spectra of S 2p for BTz-TP-COF before and after photocatalysis.

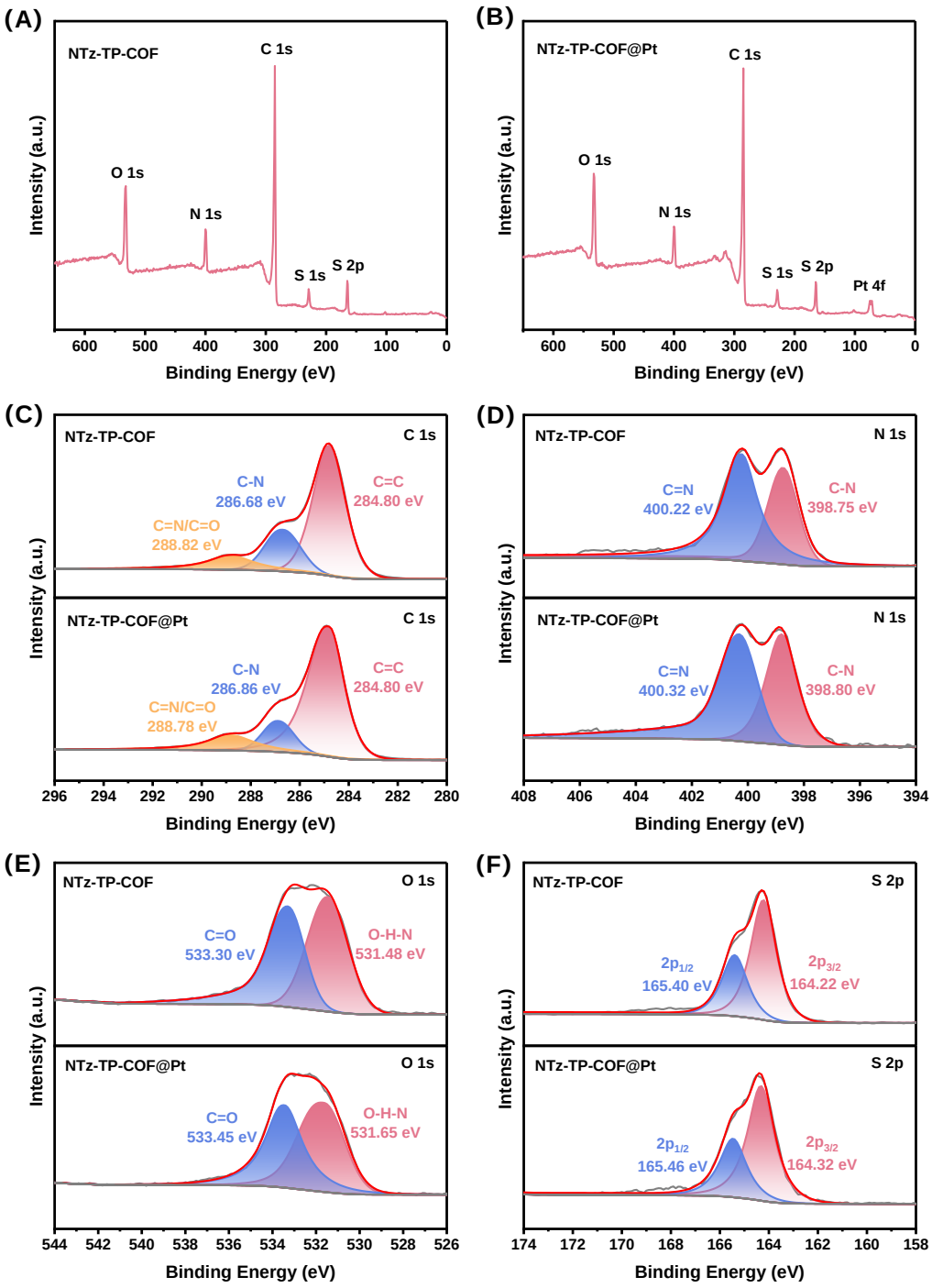

Fig. S43. (A) XPS survey spectra of NTz-TP-COF before photocatalysis. (B) XPS survey spectra of NTz-TP-COF after photocatalysis. (C) High resolution XPS spectra of C 1s for NTz-TP-COF before and after photocatalysis. (D) High resolution XPS spectra of N 1s for NTz-TP-COF before and after photocatalysis. (E) High resolution XPS spectra of O 1s for NTz-TP-COF before and after photocatalysis. (F) High resolution XPS spectra of S 2p for NTz-TP-COF before and after photocatalysis.

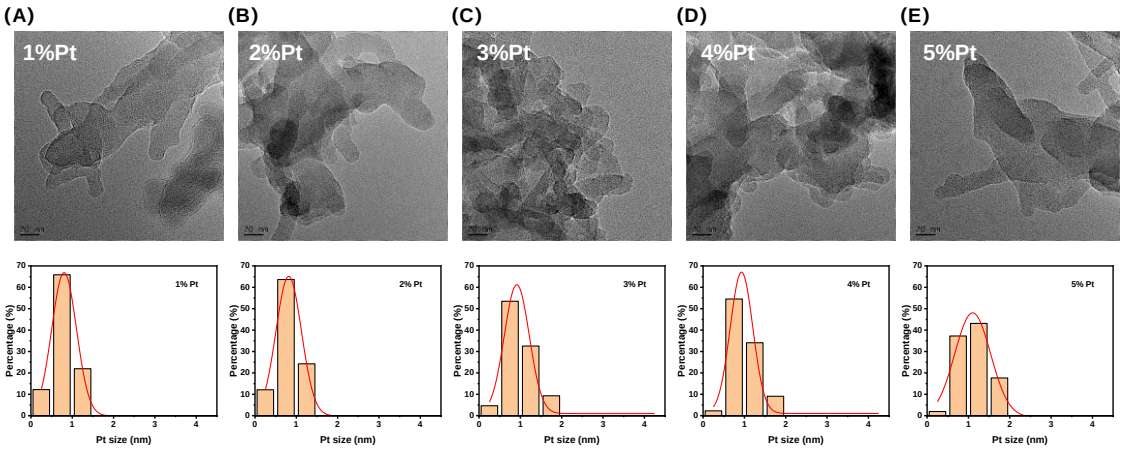

Fig. S44. HR-TEM images and photodeposited NPs size distributions of Tz-TP-COF at the Pt content of 1 wt%(A), 2 wt%(B), 3 wt%(C), 4 wt%(D), 5 wt%(E).

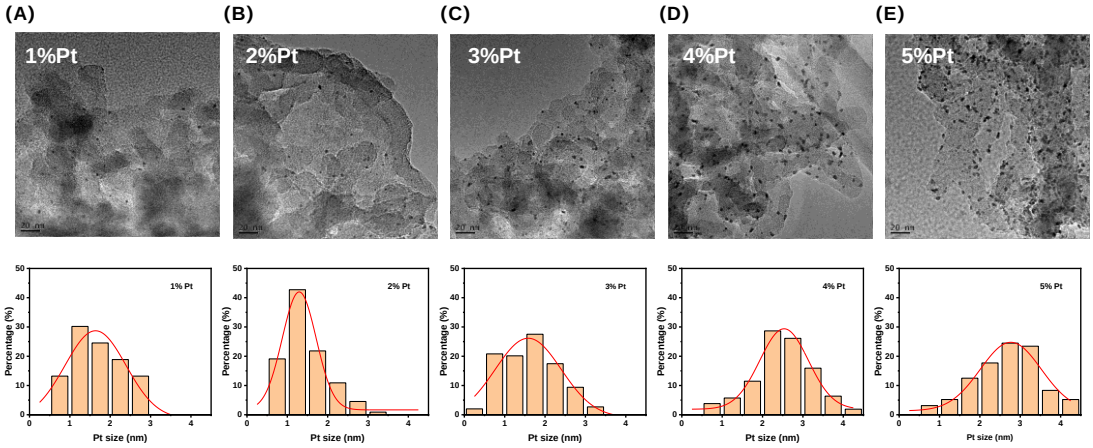

Fig. S45. HR-TEM images and photodeposited NPs size distributions of BTz-TP-COF at the Pt content of 1 wt%(A), 2 wt%(B), 3 wt%(C), 4 wt%(D), 5 wt%(E).

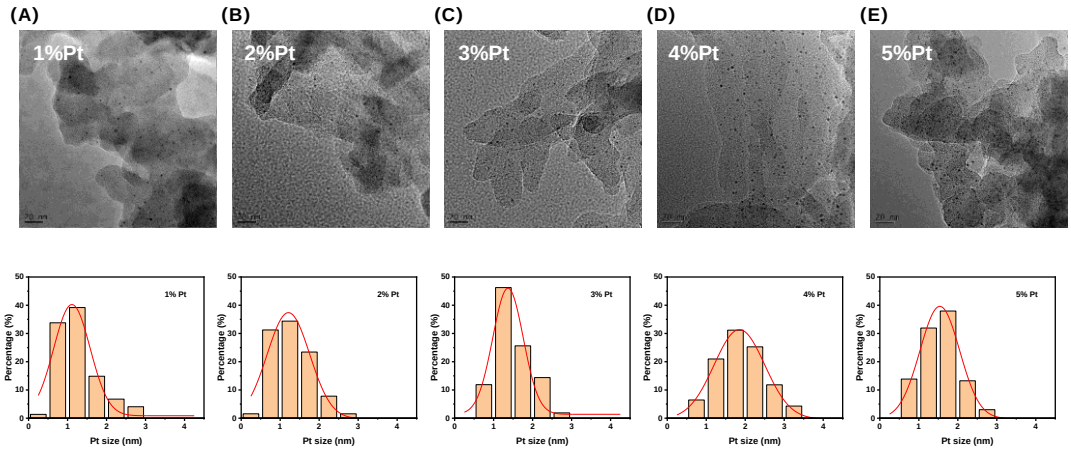

Fig. S46. HR-TEM images and photodeposited NPs size distributions of NTz-TP-COF at the Pt content of 1 wt%(A), 2 wt%(B), 3 wt%(C), 4 wt%(D), 5 wt%(E).

Table S2. Atomic coordinates of the simulated Tz-TP-COF based on AA-stacking mode.

Space group		**P1**	
Cell parameters		**a = 26.0822, b = 25.2521, c = 3.6479 α = 88.6801, β = 91.1397, γ = 120.1965**	
atoms	**x**	**y**	**z**
C1	0.08868	-0.79272	0.44757
S2	0.12887	-0.82868	0.51076
C3	0.18972	-0.76128	0.38209
C4	0.17665	-0.71586	0.29889
N5	0.11913	-0.73376	0.33675
C6	0.22094	-0.65353	0.17759
N7	0.27745	-0.63705	0.11087
C8	0.30832	-0.57762	0.01
S9	0.26976	-0.53943	-0.00712
C10	0.20896	-0.60664	0.12454
N11	0.02621	-0.82399	0.4983
N12	0.36976	-0.54793	-0.0743
C13	0.46009	-0.55434	-0.15084
C14	0.4911	-0.58926	-0.0734
C15	0.5535	-0.56466	-0.19122
C16	0.588	-0.49901	-0.29729
C17	0.56124	-0.45996	-0.26446
C18	0.49636	-0.49083	-0.29612
O19	0.47385	-0.46468	-0.45754
C20	0.59242	-0.39927	-0.20455
O21	0.63657	-0.47851	-0.43777
C22	0.58022	-0.5986	-0.19464
O23	0.46614	-0.63643	0.10971
C24	0.40189	-0.58047	-0.07007

C25	0.68606	-0.30348	-0.03564
S26	0.76056	-0.26498	0.05293
C27	0.75487	-0.20143	0.11587
C28	0.69779	-0.21251	0.06929
N29	0.65861	-0.27063	-0.01761
C30	0.68073	-0.16559	0.11134
N31	0.7204	-0.10706	0.18525
C32	0.69325	-0.07399	0.20683
S33	0.6182	-0.11292	0.13929
C34	0.62342	-0.17685	0.07795
N35	0.65484	-0.36695	-0.11919
N36	0.72532	-0.00998	0.27571
C37	0.57999	-0.69458	-0.01446
S38	0.54517	-0.77258	0.01957
C39	0.61163	-0.7639	0.1632
C40	0.6558	-0.7034	0.18142
N41	0.63778	-0.66398	0.07937
C42	0.71704	-0.68305	0.30237
N43	0.73586	-0.72237	0.38984
C44	0.79356	-0.69149	0.48623
S45	0.82718	-0.61345	0.47373
C46	0.76048	-0.62246	0.33393
N47	0.54941	-0.66365	-0.12995
N48	0.82532	-0.722	0.58283
C49	0.82622	-0.81844	0.56591
C50	0.79455	-0.88548	0.63434
C51	0.82123	-0.92241	0.52185
C52	0.88634	-0.88985	0.47068
C53	0.92161	-0.82249	0.50706
C54	0.88943	-0.78876	0.45873

O55	0.91452	-0.73807	0.3135
C56	0.98081	-0.79108	0.56129
O57	0.90992	-0.91808	0.3684
C58	0.78906	-0.98309	0.45659
O59	0.74822	-0.90936	0.80453
C60	0.79682	-0.78761	0.60194
H61	0.23379	-0.75514	0.3663
H62	0.16584	-0.61148	0.16677
H63	0.00633	-0.86922	0.59593
H64	0.39112	-0.50041	-0.10554
H65	0.56823	-0.37455	-0.19653
H66	0.62733	-0.57588	-0.25577
H67	0.37871	-0.62812	0.02192
H68	0.79222	-0.15726	0.18765
H69	0.58563	-0.22136	0.0178
H70	0.67904	-0.38953	-0.09254
H71	0.70073	0.01226	0.26987
H72	0.61799	-0.80199	0.23668
H73	0.75342	-0.58443	0.27322
H74	0.50404	-0.69053	-0.18553
H75	0.87012	-0.69459	0.6527
H76	1.00343	-0.74122	0.55692
H77	0.81263	-1.00705	0.39297
H78	0.74939	-0.81353	0.65457

Table S3. Atomic coordinates of the simulated BTz-TP-COF based on AA-stacking mode.

Space group		**P1**	
Cell parameters		**a = 28.5869, b = 28.8170, c = 3.6127 α = 90.0126, β = 91.0598, γ = 120.8772**	
atoms	**x**	**y**	**z**
C1	0.67295	-0.21733	0.15998
C2	0.72185	-0.21593	0.13046
C3	0.77173	-0.16895	0.21212
C4	0.77016	-0.12336	0.32577
C5	0.72119	-0.12491	0.35729
C6	0.67136	-0.17183	0.27489
S7	0.61786	-0.2783	0.0447
C8	0.6632	-0.2996	-0.03712
N9	0.71647	-0.26265	0.01858
N10	0.72646	-0.07824	0.4685
C11	0.77972	-0.04111	0.52057
S12	0.82527	-0.06198	0.43453
N13	0.79642	0.01277	0.62988
N14	0.64641	-0.3533	-0.15389
C15	0.49299	-0.5436	-0.42629
C16	0.53306	-0.5599	-0.51052
C17	0.59167	-0.52195	-0.43461
C18	0.61001	-0.46411	-0.44033
C19	0.57296	-0.44601	-0.31025
C20	0.51442	-0.4879	-0.27819
O21	0.48482	-0.47716	-0.10539
C22	0.58996	-0.39465	-0.20425
O23	0.65426	-0.43246	-0.56882
C24	0.62794	-0.53745	-0.35883

O25	0.51811	-0.60287	-0.66843
C26	0.43925	-0.57972	-0.47579
C27	0.16812	-0.67639	0.02847
C28	0.16898	-0.72379	0.06144
C29	0.21561	-0.72584	-0.01722
C30	0.26146	-0.67792	-0.13117
C31	0.26047	-0.6306	-0.16614
C32	0.21388	-0.62854	-0.08702
S33	0.10746	-0.68342	0.14104
C34	0.0857	-0.75026	0.22819
N35	0.12217	-0.76589	0.17449
N36	0.30735	-0.5884	-0.27713
C37	0.34406	-0.60384	-0.3254
S38	0.32255	-0.67054	-0.23584
N39	0.39807	-0.56577	-0.43404
N40	0.03206	-0.78809	0.34632
C41	0.7205	-0.71346	0.14753
C42	0.77031	-0.6658	0.12795
C43	0.77398	-0.61712	0.0295
C44	0.72514	-0.61857	-0.04922
C45	0.67535	-0.66625	-0.02953
C46	0.67168	-0.7149	0.06916
S47	0.72601	-0.76731	0.27028
C48	0.79554	-0.72318	0.28892
N49	0.81307	-0.67115	0.20889
N50	0.63258	-0.66099	-0.11179
C51	0.65004	-0.60904	-0.19374
S52	0.71954	-0.5648	-0.17362
N53	0.61198	-0.59274	-0.28755
N54	0.83346	-0.73973	0.38119

C55	0.87061	-0.88998	0.63004
C56	0.92835	-0.84945	0.71819
C57	0.94918	-0.79165	0.64922
C58	0.90908	-0.7743	0.66077
C59	0.85253	-0.81182	0.52543
C60	0.83533	-0.86973	0.48463
O61	0.79376	-0.89977	0.3069
C62	0.8175	-0.79559	0.42306
O63	0.92241	-0.73039	0.79686
C64	1.00134	-0.7553	0.57079
O65	0.95735	-0.86333	0.87431
C66	0.85271	-0.94301	0.67411
H67	0.80994	-0.16781	0.18681
H68	0.63315	-0.17294	0.29921
H69	0.7656	0.02114	0.67986
H70	0.67725	-0.3625	-0.16052
H71	0.55906	-0.3851	-0.13104
H72	0.67064	-0.50599	-0.32329
H73	0.4265	-0.62101	-0.55741
H74	0.21633	-0.76283	0.0111
H75	0.21322	-0.59151	-0.11399
H76	0.40687	-0.52644	-0.48591
H77	0.02191	-0.82844	0.34857
H78	0.81293	-0.57992	0.01446
H79	0.63273	-0.75212	0.08379
H80	0.57093	-0.62279	-0.26976
H81	0.87453	-0.70951	0.37155
H82	0.77594	-0.8265	0.34538
H83	1.01241	-0.71331	0.53828
H84	0.88198	-0.95488	0.75462

Table S4. Atomic coordinates of the simulated NTz-TP-COF based on AA-stacking mode.

Space group		**P1**	
Cell parameters		**a = 30.1323, b = 29.4349, c = 3.6323 α = 90.0695, β = 89.9305, γ = 119.9077**	
atoms	**x**	**y**	**z**
C1	0.82194	0.79448	0.0117
C2	0.77438	0.79251	-0.02763
C3	0.72804	0.74503	0.04606
C4	0.73137	0.7012	0.15588
C5	0.77792	0.70348	0.19045
C6	0.82366	0.74962	0.12022
C7	0.68045	0.74296	0.00615
C8	0.67865	0.78766	-0.10454
C9	0.72434	0.83374	-0.17582
C10	0.77099	0.83629	-0.13907
S11	0.77296	0.64561	0.31974
C12	0.70795	0.62075	0.32381
N13	0.69128	0.65407	0.23281
N14	0.811	0.88342	-0.21877
C15	0.79423	0.91645	-0.31483
S16	0.72897	0.89114	-0.31146
N17	0.67334	0.56736	0.41182
N18	0.82963	0.96941	-0.40937
C19	0.4886	0.42383	0.49543
C20	0.50465	0.3856	0.60079
C21	0.55907	0.4003	0.57198
C22	0.59671	0.45635	0.60856
C23	0.58386	0.49566	0.46675
C24	0.52931	0.47686	0.37839

O25	0.51859	0.50409	0.1869
O26	0.63676	0.46934	0.7698
O27	0.47369	0.34375	0.73765
C28	0.61882	0.54627	0.398
C29	0.57556	0.36611	0.50766
C30	0.43839	0.40901	0.49931
C31	0.20406	0.37329	-0.10536
C32	0.20372	0.32518	-0.09089
C33	0.24823	0.32397	0.02633
C34	0.29154	0.37147	0.12506
C35	0.29132	0.41809	0.1096
C36	0.24817	0.42001	-0.00475
C37	0.24776	0.27579	0.04248
C38	0.2034	0.22901	-0.05404
C39	0.16024	0.23097	-0.16789
C40	0.16033	0.27769	-0.1881
S41	0.34762	0.4708	0.24024
C42	0.36913	0.42748	0.31251
N43	0.33599	0.37659	0.24107
N44	0.11593	0.2727	-0.30382
C45	0.08226	0.22186	-0.36929
S46	0.10349	0.17821	-0.29061
N47	0.41982	0.44477	0.43597
N48	0.03167	0.2061	-0.48904
C49	0.62196	0.16781	-0.06039
C50	0.66797	0.21622	-0.02992
C51	0.66662	0.26203	0.07875
C52	0.61884	0.25727	0.15462
C53	0.57427	0.2099	0.12215
C54	0.57483	0.16471	0.01515

C55	0.7126	0.3105	0.1073
C56	0.75968	0.31367	0.02899
C57	0.76026	0.26844	-0.07623
C58	0.71577	0.22094	-0.10471
S59	0.52078	0.21307	0.22286
C60	0.56104	0.27846	0.30784
N61	0.61152	0.29661	0.26147
N62	0.72316	0.18143	-0.20595
C63	0.77355	0.19941	-0.25337
S64	0.81372	0.26534	-0.17784
N65	0.54189	0.31191	0.41658
N66	0.79145	0.16455	-0.35486
C67	0.84763	0.05605	-0.58245
C68	0.90309	0.07716	-0.63229
C69	0.93944	0.13245	-0.53654
C70	0.9175	0.16518	-0.40696
C71	0.86263	0.14799	-0.46886
C72	0.8295	0.09388	-0.60764
O73	0.78869	0.08077	-0.75774
O74	0.94349	0.20458	-0.22493
O75	0.91866	0.05033	-0.77734
C76	0.845	0.18072	-0.37853
C77	0.99025	0.15029	-0.55849
C78	0.814	0.0054	-0.51041
H79	0.85739	0.83055	-0.0433
H80	0.85983	0.75045	0.14855
H81	0.64501	0.70689	0.06126
H82	0.64246	0.78673	-0.13462
H83	0.68953	0.54361	0.44872
H84	0.86826	0.98083	-0.37868

H85	0.60485	0.57208	0.30725
H86	0.61671	0.3813	0.49965
H87	0.41059	0.36832	0.55959
H88	0.17032	0.37448	-0.19502
H89	0.24909	0.45723	-0.01667
H90	0.28147	0.27456	0.13231
H91	0.20227	0.1917	-0.03888
H92	0.44278	0.48475	0.49045
H93	0.02323	0.23591	-0.53922
H94	0.6227	0.1328	-0.14429
H95	0.53923	0.12795	-0.01012
H96	0.71188	0.34554	0.19069
H97	0.79527	0.3505	0.05175
H98	0.50222	0.29566	0.40667
H99	0.76348	0.12503	-0.36587
H100	0.87279	0.22047	-0.29559
H101	1.00311	0.12277	-0.62971
H102	0.77361	-0.00628	-0.4935

Section III. Supplementary References

1. Y. Xu, Y. Lang, N. Sun, X. Ci, R. Tu, C. Yang, X. Fang, T. Liu, L. Yang, C.-C. Liu, W.-Q. Deng and Z. Li, *ACS Catal.*, 2025, **15**, 18976-18986.
2. X. A. Li, Z. Z. Liang, Y. C. Zhou, J. F. Huang, X. L. Wang, L. M. Xiao and J. M. Liu, *Aggregate*, 2024, **5**, e442.
3. W. Huang, Y. Hu, Z. Qin, Y. Ji, X. Zhao, Y. Wu, Q. He, Y. Li, C. Zhang, J. Lu and Y. Li, *Natl. Sci. Rev.*, 2023, **10**, nwac171.
4. F. Liu, Y. He, X. Liu, Z. Wang, H.-L. Liu, X. Zhu, C.-C. Hou, Y. Weng, Q. Zhang and Y. Chen, *ACS Catal.*, 2022, **12**, 9494-9502.
5. A. F. Saber, H.-T. Liao, P.-J. Li, Y.-F. Chen, L. Mabuti, S.-W. Kuo, J. Lüder and A. F. M. El-Mahdy, *J. Colloid Interface Sci.*, 2025, **699**, 138156.
6. Z. Jia, N. Ji, J. Qi, T. Wang, Y. Che, Z. Zhao, J. Zhao, Z. Jiao, K. Wang, W. Zhang and W. H. Zhu, *Angew. Chem. Int. Ed.*, 2025, **64**, e202511245.
7. H. Wang, L. Shi, Z. Qu, L. Zhang, X. Wang, Y. Wang, S. Liu, H. Ma and Z. Guo, *ACS Appl. Mater. Interfaces*, 2024, **16**, 2296-2308.
8. Y. Chen, F. Duan, J. Zhang, S.-C. Xu, S.-B. Ren, L. Zhang and D.-M. Han, *ACS Appl. Mater. Interfaces*, 2025, **17**, 29504-29514.
9. H. Hou, K. Wu, X. Chen, X. Liu and Y. Zhao, *J. Am. Chem. Soc.*, 2025, **147**, 27835-27846.
10. Y. Hu, X. Ding, J. Feng, Y. Yan, C. Shao, X. Yu, J. Shao, Y. Ji, Y. Li, W. Huang and Y. Li, *Adv. Funct. Mater.*, 2024, **34**, 2400946.
11. S. A. Z. Naqvi, A. U. R. Baloch, U. Y. Umna, K. Muzaffar, T. S. Aslam, J. Chen and Y. Wang, *J. Mater. Chem. A*, 2025, **13**, 30419-30426.
12. H. Wang, L. Guan, J. Liu, T. Lei, Y. Xue, Z. Qu, S. Jin, H. Ma and Z. Guo, *J. Mater. Chem. A*, 2022, **10**, 16328-16336.
13. Y. Wang, W. Hao, H. Liu, R. Chen, Q. Pan, Z. Li and Y. Zhao, *Nat. Commun.*, 2022, **13**, 100.
14. M. Wang, Z. Wang, M. Shan, J. Wang, Z. Qiu, J. Song and Z. Li, *Chem. Mater.*, 2023, **35**, 5368-5377.
15. Y. Chen, X. Luo, J. Zhang, L. Hu, T. Xu, W. Li, L. Chen, M. Shen, S.-B. Ren, D.-M. Han, G.-H. Ning and D. Li, *J. Mater. Chem. A*, 2022, **10**, 24620-24627.
16. Z. Qu, S. Liu, Y. Wang, J. Yang, Y. Zhang, J. Zhang, Y. Gao, H. Ma and Z. Guo, *ACS Appl. Polym. Mater.*, 2024, **6**, 4756-4768.
17. H. Yu, J. Zhang, X. Yan, C. Wu, X. Zhu, B. Li, T. Li, Q. Guo, J. Gao, M. Hu and J. Yang, *J. Mater. Chem. A*, 2022, **10**, 11010-11018.
18. S. Li, R. Ma, S. Xu, T. Zheng, H. Wang, G. Fu, H. Yang, Y. Hou, Z. Liao, B. Wu, X. Feng, L.-Z. Wu, X.-B. Li and T. Zhang, *ACS Catal.*, 2023, **13**, 1089-1096.
19. K. Wang, Z. Jia, Y. Bai, X. Wang, S. E. Hodgkiss, L. Chen, S. Y. Chong, X. Wang, H. Yang, Y. Xu, F. Feng, J. W. Ward and A. I. Cooper, *J. Am. Chem. Soc.*, 2020, **142**, 11131-11138.
20. X.-L. Wang, X.-R. Ren, Z. Xu, P.-K. Zhou, Z.-Y. Li and D. Wang, *ACS Appl. Polym. Mater.*, 2026, **8**, 3459-3465.
21. W. Li, X. Huang, T. Zeng, Y. A. Liu, W. Hu, H. Yang, Y. B. Zhang and K. Wen, *Angew. Chem. Int. Ed.*, 2020, **60**, 1869-1874.
22. M. Mohamed Samy, I. M. A. Mekhemer, M. G. Mohamed, M. Hammad Elsayed, K.-H. Lin, Y.-K. Chen, T.-L. Wu, H.-H. Chou and S.-W. Kuo, *Chem. Eng. J.*, 2022, **446**, 137158.
23. B. P. Biswal, H. A. Vignolo-González, T. Banerjee, L. Grunenberg, G. Savasci, K. Gottschling, J. Nuss, C. Ochsenfeld and B. V. Lotsch, *J. Am. Chem. Soc.*, 2019, **141**, 11082-11092.